

Pillar[5]arene-Based Polycationic Glyco[2]rotaxanes Designed as *Pseudomonas aeruginosa* Antibiofilm Agents

Tharwat Mohy El Dine, Ravikumar Jimmidi, Andrei Diaconu, Maude Fransolet, Carine Michiels, Julien De Winter, Emilie Gillon, Anne Imberty, Tom Coenye, and Stéphane P. Vincent*



Cite This: <https://doi.org/10.1021/acs.jmedchem.1c01241>



Read Online

ACCESS |



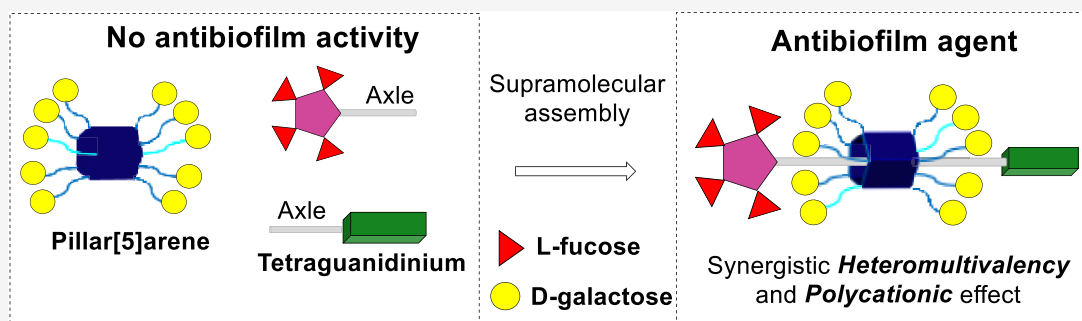
Metrics & More



Article Recommendations



Supporting Information



ABSTRACT: *Pseudomonas aeruginosa* (P.A.) is a human pathogen belonging to the top priorities for the discovery of new therapeutic solutions. Its propensity to generate biofilms strongly complicates the treatments required to cure P.A. infections. Herein, we describe the synthesis of a series of novel rotaxanes composed of a central galactosylated pillar[5]arene, a tetra-fucosylated dendron, and a tetraguanidinium subunit. Besides the high affinity of the final glycorotaxanes for the two P.A. lectins LecA and LecB, potent inhibition levels of biofilm growth were evidenced, showing that their three subunits work synergistically. An antibiofilm assay using a double $\Delta\text{lecA}\Delta\text{lecB}$ mutant compared to the wild type demonstrated that the antibiofilm activity of the best glycorotaxane is lectin-mediated. Such antibiofilm potency had rarely been reached in the literature. Importantly, none of the final rotaxanes was bactericidal, showing that their antibiofilm activity does not depend on bacteria killing, which is a rare feature for antibiofilm agents.

INTRODUCTION

Bacterial biofilms are microbial communities held together by an extracellular matrix composed of polysaccharides, extracellular DNA (eDNA), lipids, and proteins.¹ *In vivo* biofilm formation is a major therapeutic problem for three main reasons: (i) biofilms can be associated with chronic bacterial infections (for instance, wound infections, chronic lung infections associated with cystic fibrosis, etc.);² (ii) bacteria in biofilms can be up to 3 orders of magnitude less susceptible to antibiotics compared to planktonic bacteria that grow in suspension;³ and (iii) they account for a large percentage of nosocomial infections and infections associated with implanted medical devices (e.g., catheters).⁴ Therefore, there is an urgent need for new agents to inhibit biofilm formation. Ideally, such antibiofilm molecules should not affect bacterial cell viability to preserve the natural bacterial flora and avoid selective pressure leading to the development of resistance. Among the different pathogens that have acquired resistance to classical antibiotics, *Pseudomonas aeruginosa*, which is an important opportunistic Gram-negative bacterial pathogen,⁵ was listed as a critical priority 1 pathogen by the WHO in 2017. *P. aeruginosa* can cause acute or chronic airway infections that can be lethal in immuno-compromised, cystic fibrosis, and cancer patients, and

it is an important wound pathogen, and in many cases, *P. aeruginosa* infections are biofilm-related.⁶

In 2008, the team of Reymond and collaborators described glycopeptide dendrimers capable of inhibiting *P. aeruginosa* biofilm formation as well as dispersing established *P. aeruginosa* biofilms.⁷ These multivalent molecules were initially prepared in a combinatorial manner and screened against bacterial lectins specific for L-fucose. From initial screening, the biological activities were then improved by modifying the dendritic peptide scaffold and also by targeting another *P. aeruginosa* lectin.⁸ In the latter case, the dendrimers were decorated with D-galactosides and Lewis^a derivatives. The two *P. aeruginosa* lectins involved in the formation of biofilms are LecA and LecB.⁹ LecA, which selectively binds D-galactose, plays an important role in *P. aeruginosa* virulence.¹⁰ It is also involved in biofilm formation during chronic infections.¹¹ LecB

Received: July 12, 2021

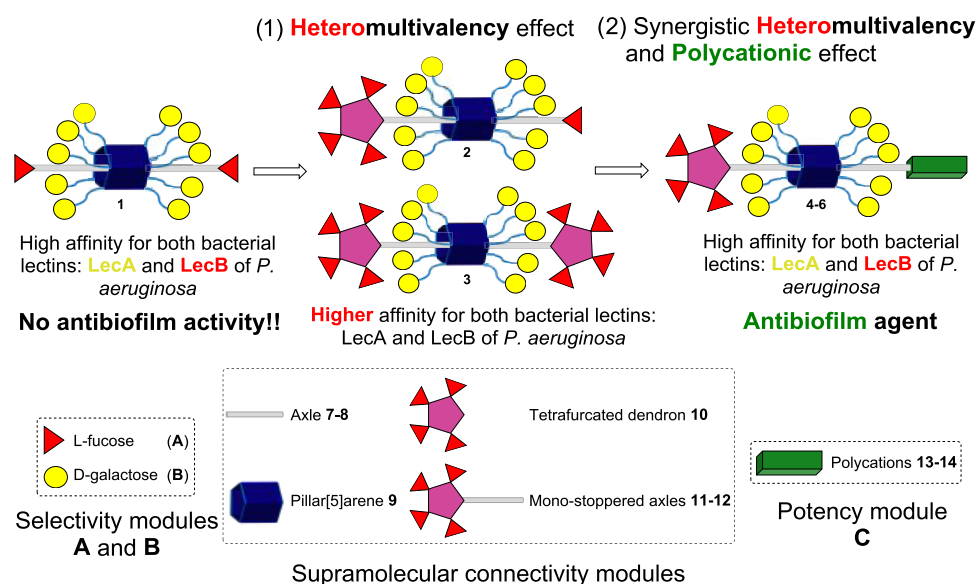


Figure 1. Design principles underlying this study. Glycorotaxane **1** is a potent ligand of *Pseudomonas aeruginosa* lectins LecA and LecB¹⁶ but has no antibiofilm activity. The novel rotaxanes targeted in the present work address the effect of (1) multivalent fucose presentation (rotaxanes 2–3) and (2) the presence of a polycationic subunit on the axle (rotaxanes 4–6) on the observed antibiofilm activity.

binds L-fucose and also contributes to biofilm formation.¹² It is believed that the tetrameric structure of these two lectins allows them to cross-link the bacterial biofilm polysaccharides and the host cells.¹³ In addition, Vidal et al. clearly showed that developing glycoclusters that tightly bind LecA and/or LecB does not necessarily lead to antibiofilm agents.^{18g}

Recently, polycationic species of controlled structures were synthesized and showed very promising antibiofilm activities against Gram-positive bacteria, but were ineffective against Gram-negative bacteria, including *P. aeruginosa*.¹⁴ These molecules were constructed on a pillar[*n*]arene scaffold, and it was shown that cationic groups, their number, as well as their accessibility play a critical role in the antibiofilm process. Later on, a novel generation of bactericidal pillar[5]arene nanoaggregates was shown to disrupt *Escherichia coli* biofilms.¹⁵ These polycationic bactericides have no functional elements (such as a sugar) that could provide selectivity toward specific pathogenic bacteria. Mechanistically, they are hypothesized to target the eDNA in the biofilm matrix, resulting in the disruption of this matrix and/or prevention of host–pathogen interaction by polyelectrostatic and hydrophobic interactions. These polycations are interesting candidates as antibacterial/antibiofilm agents, but their lack of selectivity is likely problematic for *in vivo* applications. To summarize, literature data clearly indicate that some antibiofilm activities can be achieved through the multivalent presentation of either specific carbohydrates or cationic species.

We have recently disclosed the synthesis of glycorotaxane **1** bearing 10 β -galactosides and 2 α -fucosides as a potent ligand of the two lectins, LecA and LecB,¹⁶ of *P. aeruginosa* (Figure 1). Thanks to its multivalent nature, glycorotaxane **1** is a strong ligand of both lectins LecA and LecB.¹⁶ However, as will be shown below, this heterovalent glycocluster was found to be unable to inhibit *P. aeruginosa* biofilm formation *in vitro*. To develop potent biofilm inhibitors, we aimed to engineer novel heteromultivalent glycorotaxanes of general structures 2–6 (Figure 1).

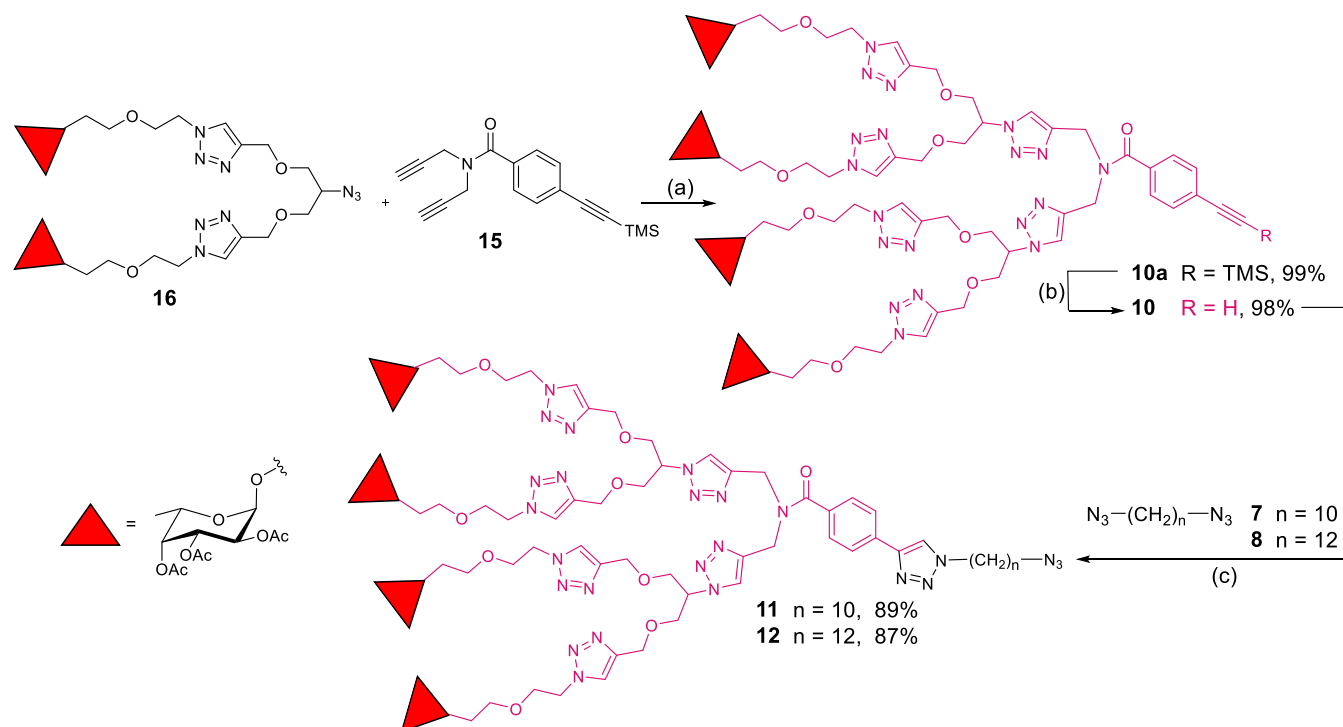
Many monovalent or multivalent fucosides and galactosides are indeed potent LecA or LecB ligands, but their antibiofilm

powers have rarely been evaluated.¹⁷ In some cases, weak to moderate antibiofilm properties could be measured.^{13a,18} More recently, carbohydrate–antibiotic conjugates were designed as LecA and LecB ligands: interestingly, they were found to accumulate in *P. aeruginosa* biofilm without being antibiofilm.^{13b}

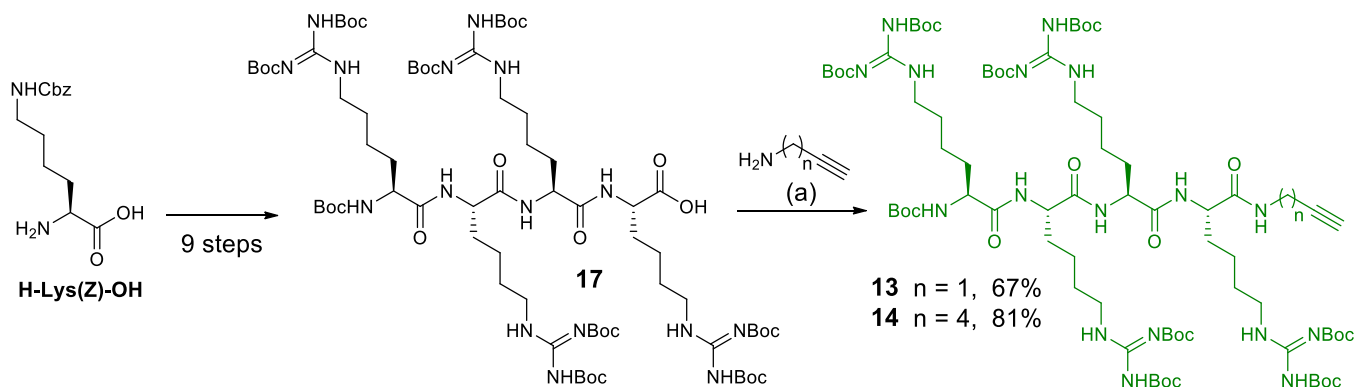
Inspired by the above-mentioned seminal results obtained by Raymond^{8a–c,7a} with glycopeptides and by Cohen and Fridman¹⁴ with polycationic pillars, we designed a new generation of rotaxanes 2–6 displayed in Figure 1. We reasoned that glycorotaxane **1** failed to inhibit biofilm formation either because of the lack of multivalency for the fucosidic subunit “cluster effect”¹⁹ or because a polycationic subunit (that we coin a “potency module” in this study) is missing in the structure. Keeping the pillar[5]arene bearing 10 galactosides as the common core structure, we designed glycorotaxanes 2–3 with one or two tetrafurcated dendrons and glycorotaxanes 4–6 with a polycationic tail. As small structural differences in the spacers may sometimes trigger huge differences in the biological activity of glycoclusters,²⁰ we designed three cationic heteroglycoclusters 4–6 with three different central chain lengths.

As pointed by most of the above-mentioned antibiofilm studies, it is crucial to identify strategies and design molecules capable of mechanistically preventing or inhibiting *P. aeruginosa* biofilm formation without affecting the bacterial cell viability and growth to prevent possible evolutionary trajectories toward antibiotic resistance.^{8c,14,21}

Herein, we describe the synthesis of a series of rotaxanes bearing multivalent displays of fucosides and galactosides and a polycationic tail, their biophysical characterization as LecA and LecB ligands, as well as their antibiofilm properties. The goal of the present study is to demonstrate that potent *P. aeruginosa* antibiofilm activity requires synergistic action of the saccharidic and the polycationic subunits of the rotaxanes. The non-bactericidal effect of the final rotaxanes as well as their lack of detectable membrane damage to red blood cells and toxicity to human lung cells *in vitro* was also evaluated.

Scheme 1. Synthesis of the First Selectivity Subunit 10 and the [2]Rotaxane Threads 11–12^a

^aReaction conditions: (a) CuSO_4 , Na-ascorbate, $t\text{-BuOH}/\text{H}_2\text{O}$, 60 °C, 12 h; (b) TBAF·3H₂O, THF, 0 °C, 5 min; (c) CuBr·SMe₂, CHCl₃, 20 °C, 12 h.

Scheme 2. Synthesis of the Potency Subunits 13 and 14^a

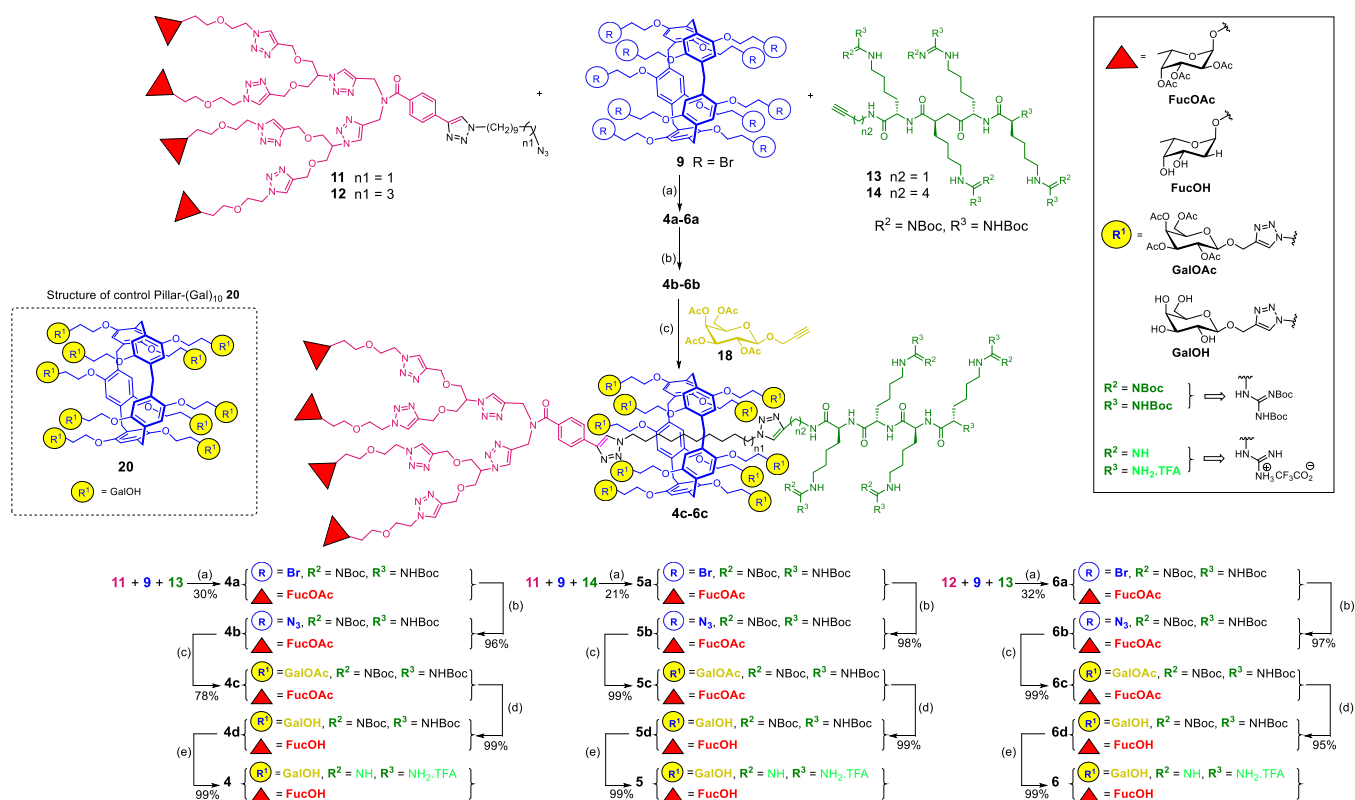
^aReaction conditions: (a) HOBt, EDCl, CH₂Cl₂, 0–20 °C, 12 h.

RESULTS AND DISCUSSION

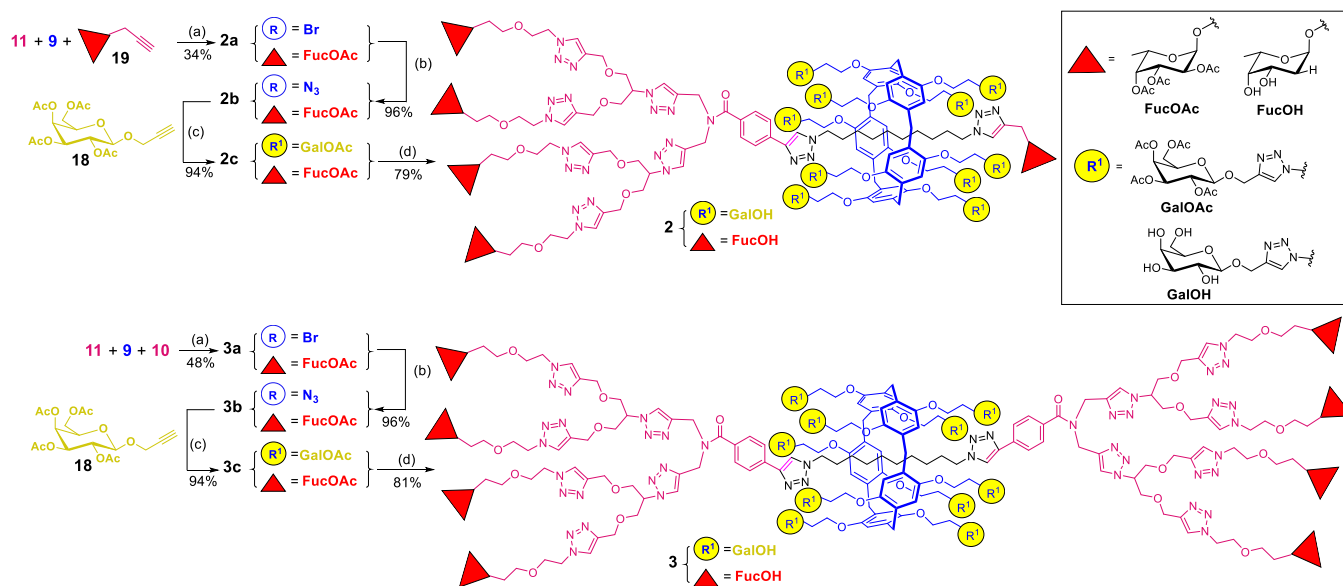
Design and Synthesis of Glycorotaxanes 2–6.

Heterovalency was easily achieved thanks to the noncovalent mechanical bond of the central axle (7 or 8) linking the selectivity module (10), the potency module (13 or 14), and the central pillar[5]arene (9). This supramolecular approach avoids the cumbersome regioselective synthesis of heterovalent multimers (Figure 1). Modules A and B are two handles to achieve a strong and selective binding to a given bacterium species while the potency module C will insure the antibiofilm power. Thanks to the rotaxane supramolecular technology, three distinct subunits can be selectively assembled in one complex heteromeric structure, without the need of selective protections–deprotections of a given central scaffold.

Accordingly, we started with the synthesis of the first selectivity subunit 10, and the [2]rotaxane mono-stoppered threads 11–12 (Scheme 1). Tris-alkyne 15 and divalent fucoside 16 were primarily prepared in six and ten steps, respectively (Schemes S4–S6, SI). Using these two building blocks, the protected tetravalent fucoside 10a was obtained under Cu(I)-assisted azide–alkyne cycloaddition (CuAAC) conditions. Desilylation of the latter provided 10 which was further treated with 7 or 8 (Scheme 1; also Schemes S1 and S4–S8, SI) using the CuAAC reaction to furnish threads 11 and 12 in 89 and 87% yields, respectively. The second selectivity subunit consisting of deca-brominated pillar[5]arene 9 was generated in two steps according to a literature procedure (Scheme S2, SI).²²

Scheme 3. Synthesis of Polycationic Heteroglyco[2]rotaxanes 4–6^a

^aReaction conditions: (a) CuBr·SMe₂, CHCl₃, -20 to 20 °C, 15 h; (b) NaN₃, DMF, 20 °C, 24 h; (c) CuSO₄·5H₂O, Na-ascorbate, CH₂Cl₂/H₂O, 20 °C, 24 h; (d) NaOMe, MeOH/CHCl₃, 0–20 °C, 4 h; (e) TFA, CH₂Cl₂, 20 °C, 4 h.

Scheme 4. Synthesis of Heteroglyco[2]rotaxanes 2–3^a

^aReaction conditions: (a) CuBr·SMe₂, CHCl₃, -20 to 20 °C, 15 h; (b) NaN₃, DMF, 20 °C, 24 h; (c) CuSO₄·5H₂O, Na-ascorbate, CH₂Cl₂/H₂O, 20 °C, 24 h; (d) NaOMe, MeOH/CHCl₃, 0–20 °C, 4 h.

The potency subunits 13–14 which are required for achieving enhanced antibiofilm activity consisted of a clickable polypeptidic chain bearing four guanidinium groups. *N*-Boc-protected tetrapeptide 17 was prepared in nine steps starting from *N*-Cbz-*L*-lysine (Schemes S9 and S10, SI). Amide

coupling of 17 with propargyl or hexyl amine in the presence of EDCI/HOBt afforded 13 and 14 in 67 and 81% yields, respectively (Scheme 2; also see Scheme S11, SI).

A family of heteroglycoclusters 4–6 incorporating the potency subunits on their mono-stoppered threads was

Table 1. ITC Data for the Bindings of LecA and LecB to Heteroglyco[2]rotaxanes 1–6 and to Reference Compounds β -D-GalOMe, α -L-FucOMe, Deacetylated Mono-stoppered Thread 11, and (Pillar[5]arene with (GalOH)₁₀) 20^a

ligand	n_{sugar}^b	lectin	n'^c	N^d	K_d [nM]	$-G$ [kJ mol ⁻¹]	$-\Delta H$ [kJ mol ⁻¹]	$-T\Delta S$ [kJ mol ⁻¹]	rp/n_{sugar}^e
β -D-GalOMe ^f	1	LecA	1		55 700	24.3	19.0	5.3	
α -L-FucOMe ^g	1	LecB	0.77		430	36.4	41.3	4.9	
11 (Fuc) ₄ N ₃	4	LecB	0.19 ± 0.02	5	150 ± 10	39.1 ± 0.2	144.0 ± 0	104.5 ± 0.5	0.72
20 Pillar (GalOH) ₁₀	10	LecA	0.16 ± 0.01	6	145 ± 10	39.1 ± 0.1	157.0 ± 3	118.0 ± 3	38
1 (Gal) ₁₀ (Fuc) ₂	10	LecA	0.22 ± 0.004	4–5	646 ± 10	35.4 ± 3.7	105.0 ± 3.5	69.4 ± 15	8.6
	2	LecB	0.65 ± 0.004	1–2	474 ± 40	36.1 ± 2	61.6 ± 0.8	25.4 ± 15	0.45
2 (Gal) ₁₀ (Fuc) ₅ (subunits 11, 9, and 19)	10	LecA	0.26 ± 0.01	4	230 ± 40	37.9 ± 0.4	71.0 ± 4	33.0 ± 5	24
	5	LecB	0.20 ± 0.004	5	160 ± 30	39.0 ± 0.5	138.0 ± 5	99.0 ± 4	0.67
3 (Gal) ₁₀ (Fuc) ₈ (subunits 11, 9, and 10)	10	LecA	0.21 ± 0.01	4–5	770 ± 50	34.9 ± 0.2	68.6 ± 1.7	33.0 ± 1.7	7.2
	8	LecB	0.16 ± 0.01	6	160 ± 20	38.9 ± 0.4	201.0 ± 1	162.5 ± 0.5	0.34
4 (Gal) ₁₀ (Fuc) ₄ (NH ₂ ·TFA) ₅ (subunits 11, 9, and 13)	10	LecA	0.25 ± 0.01	4	150 ± 30	39.0 ± 0.4	97.5 ± 2.4	58.0 ± 3	37
	4	LecB	0.23 ± 0.02	4	130 ± 30	39.4 ± 0.7	110.0 ± 8	71.0 ± 9	0.82
5 (Gal) ₁₀ (Fuc) ₄ (NH ₂ ·TFA) ₅ (subunits 11, 9, and 14)	10	LecA	0.29 ± 0.01	3–4	170 ± 50	38.7 ± 0.8	84.7 ± 0.9	46.0 ± 1.6	33
6 (Gal) ₁₀ (Fuc) ₄ (NH ₂ ·TFA) ₅ (subunits 12, 9, and 13)	10	LecA	0.31 ± 0.01	3	226 ± 10	37.9 ± 0.1	70.3 ± 3.7	32.4 ± 3	24
	4	LecB	0.35 ± 0.06	3	171 ± 16	38.7 ± 0.82	77.7 ± 1.7	37.8 ± 0.7	0.63

^aThermodynamic parameters, dissociation constants K_d , and n' are reported as an average ± standard deviation of at least two independent ITC runs. Normal titration was used with the lectin present in the cell of VP-ITC and the ligand in the syringe. ^bValency n_{sugar} = number of copies of galactosides or fucosides in the ligand. ^cStoichiometry of the binding n' = fraction of glycocluster per lectin binding site. ^d N = number of lectin monomers bound to each cluster. ^eRelative potency per galactose or fucose residue $rp/n_{\text{sugar}} = (K_d(\text{monomeric})/K_d(\text{multimeric ligand}))/n_{\text{sugar}}$. ^fData from ref 23. ^gData from ref 24.

designed (Scheme 3). [2]Rotaxane **4a** was obtained in 30% yield from **11**, **9**, and **13** using the threading followed by stoppering approach which was performed by CuAAC reaction. Given the inability of CHCl₃ to form an inclusion complex with the pillar[5]arene **9** that would prevent the axle **11** from entering into its inner cavity, threading of **11** and further formation of [2]rotaxane **4a** was carried out in CHCl₃ at room temperature for 5 h.

Moreover, the formation of the non-interlocked di-stoppered axle was minimized by carrying out the reaction at the highest possible concentration and by lowering the temperature to -20 °C prior to the addition of the copper catalyst (Tables S1–S3, SI). Furthermore, **9** was used in large excess (8.0 equiv) along with CuBr·SMe₂ (8.0 equiv) because of the ability of guanidinium groups to complex Cu^I.

[2]Rotaxane **5a** was prepared from **11**, **9**, and **14** in 21% yield while **6a** was obtained from **12**, **9**, and **13** in 32% yield using the same previous conditions developed for the synthesis of **4a**.

Treatment of deca-brominated **4a–6a** with NaN₃ in DMF furnished deca-azides **4b–6b** in 96–98% yields (Scheme 3). Post-functionalization of the pillar[5]arene subunit of [2]-rotaxanes **4b–6b** was thereafter achieved using the CuAAC reaction with monovalent galactosides **18** to yield the corresponding heteroglycoclusters **4c–6c** in 78–99% yields. Final polycationic heteroglyco[2]rotaxanes **4–6** were then efficiently generated in excellent yields through a Zemplén deacetylation-Boc deprotection sequence.

To study the effect of heteromultivalency of glyco[2]-rotaxanes on the antibiofilm properties, penta- and octa-fucosylated heteroglyco[2]rotaxanes **2** and **3**, respectively, were synthesized (Scheme 4). These [2]rotaxanes were prepared following a similar synthetic sequence, however using smaller excess of CuBr·SMe₂ (4.0 or 6.0 equiv; also see Tables S4 and S5, SI). Treatment of **11** with the macrocyclic reagent **9** in the

presence of monovalent fucoside **19** or tetravalent fucoside, tetravalent fucoside **10** afforded [2]rotaxanes **2a** and **3a** in 34% and 48% yields, respectively. Heteroglyco[2]rotaxanes **2** and **3** (Scheme 4) were obtained in very good yields following the deca-azidation of **2a–3a** (96%), CuAAC reaction of **2b–3b** with monovalent galactose **18** (94%), and final Zemplén deacetylation of **2c–3c** (79–81%).

All of the intermediates and final glycorotaxanes were characterized by ¹H NMR, ¹³C NMR, and high-resolution mass spectrometry (HR-MS, mass accuracy measurement). Detailed synthetic procedures and characterization data of the different building blocks and scaffolds are presented in the SI. A typical shift of the signals of the aliphatic axle due to its localization inside the pillar[5]arene cavity was systematically observed by ¹H NMR. The moderate yields of the synthesized [2]rotaxanes **2a–6a** were comparable to those of similar rotaxanes reported in the literature,¹⁶ which is probably due to the steric hindrance caused by the 10 bromides present on the macrocycle.

ITC Experiments. Heteroglyco[2]rotaxanes **1–6** were evaluated as potential ligands of *P. aeruginosa* lectins, that is galactose-specific LecA and fucose-specific LecB, by isothermal titration calorimetry (ITC). Binding affinities of **1–6** to LecA and LecB were compared to those of monovalent references methyl- β -D-galactoside (β -GalOMe) and methyl- α -L-fucopyranoside (α -FucOMe), deacetylated mono-stoppered thread **11** and the deacetylated deca-galactosylated pillar[5]arene **20**. ITC data of the different ligands are outlined in Table 1. Selected sensorgrams and integration with best fit for each compound interacting with lectins are shown in Figures S1–S7, SI.

All final rotaxanes **1–6** structurally share a pillar[5]arene core bearing 10 β -galactosides. Compared to the reference methyl- β -D-galactoside ($K_d = 55\,700$ nM), binding affinities of **1–6** to the galactose-specific lectin LecA ranged between 150

nM (4) and 770 nM (3). Their relative potency per galactose unit (r.p./n) ranged from 7.2 to 37, which indicates that a multivalent effect operates for all of them and a huge gain in affinity, which is at least 100–400 times higher than monovalent galactoside was observed, in particular for glycorotaxanes 4–6 bearing the polyguanidinium tail whose potencies (r.p./n from 24 to 37) were comparable to that of the control pillar[5]arene 20 (r.p./n 38, $K_d = 145$ nM). These data clearly show that the presence of either the (tetra)-fucosidic subunit or the polycationic tail barely affects the global affinity toward LecA (K_d) and the affinity enhancement through a multivalent effect.

For the fucose-specific lectin LecB, the inclusion of one or two tetra-fucosylated moieties 10 (rotaxanes 2–6, K_d values from 130 to 171 nM) resulted in higher affinities (by a factor of 2.6–3.5) compared to the initial glycorotaxane 1 ($K_d = 474$ nM). In all cases, no multivalent effect was observed with this lectin as confirmed by the low relative potencies (r.p./nFuc < 1), a result consistent with literature data for this lectin whose ball shape with binding sites being far apart makes it less sensitive to multivalent ligands.^{8c} Compared to glycorotaxane 3 bearing two tetra-fucosides and glycorotaxane 2 bearing one tetra-fucoside, rotaxanes 4–6 displaying only one tetra-fucosylated moiety clearly demonstrated that a single tetrameric fucoside is sufficient for reaching high affinity to LecB. Importantly, the comparison of all molecules 1–6 with the tetra-fucoside 11 alone ($K_d = 150$ nM) showed that neither the presence of the deca-galactosylated pillar[5]arene nor that of the polyguanidinium tail in molecules 4–6 decreased the affinity toward LecB.

In summary, the new glycorotaxanes 2–6 showed high affinity for both *P. aeruginosa* lectins LecA and LecB with an improved affinity compared to the initial rotaxane 1. In addition, the polycationic tail in rotaxanes 4–6 did not alter their affinities toward the two lectins.

Biofilm Inhibition Assays. Antibiofilm properties were determined using the crystal violet assay which quantifies biofilm biomass through staining with crystal violet.^{14b,25} Bacteria were incubated 24 h with decreasing amounts of compounds 1–6 in twofold serial dilutions. The MBIC₅₀ value is defined as the minimal concentration at which at least 50% reduction in the biofilm biomass was measured compared to untreated cells. The results are summarized in Table 2.

Multivalent heteroglycoclusters 1–3 lacking a polycationic potency module did not inhibit the biofilm growth (Figure 2a). Replacing the mono- (19) or tetra-fucosidic (10) subunits in 2–3 by the polyguanidinium group in rotaxane 4 lead to 70% biofilm inhibition at MBIC₅₀ of 37.5 μ M. A similar effect was observed using the hexyl potency group 14 (rotaxane 5). Elongation of the aliphatic mono-stoppered axle (11 vs 12) led to a similar reduction in the biofilm formation but at a significantly lower MBIC₅₀ of 2.4 μ M (rotaxane 6). Moreover, examination of the biofilm inhibition percentages of 4–6 at MBIC₅₀ showed that these three cationic rotaxanes had a comparable antibiofilm activity.

This study has clearly provided evidence that the multivalent display of both sugars alone, as in molecules 1, 2, and 3, is not sufficient to promote antibiofilm activity. Molecules 2 and 3 did not show any activity on the biofilm formation, while molecule 1 promoted its formation at high concentrations (Figure 2a). Clearly, the presence of a polycationic module is crucial for achieving potent inhibition of biofilm formation (rotaxanes 4–6). It is interesting to note that the simple

Table 2. Inhibition of *P. aeruginosa* Biofilms by Heteroglyco[2]rotaxanes 1–6^a

compound	MBIC ₅₀ ^a μ M (μ g/mL)	inhibition at MBIC ₅₀ (%) \pm SD (SEM)	MIC, ^b μ M (μ g/mL)
1 (Gal) ₁₀ (Fuc) ₂	>150 (616.7)	n.a.	>150 (616.7)
2 (Gal) ₁₀ (Fuc) ₅ (subunits 11, 9, and 19)	>150 (844.0)	n.a.	>150 (844.0)
3 (Gal) ₁₀ (Fuc) ₈ (subunits 11, 9, and 10)	>150 (1071.1)	n.a.	>150 (1071.1)
4 (Gal) ₁₀ (Fuc) ₄ (NH ₂ ·TFA) ₅ (subunits 11, 9, and 13)	37.5 (252.4)	70 \pm 21.9 (5.2)	>150 (1009.6)
5 (Gal) ₁₀ (Fuc) ₄ (NH ₂ ·TFA) ₅ (subunits 11, 9, and 14)	37.5 (254.0)	68 \pm 15.1 (3.6)	>150 (1015.9)
6 (Gal) ₁₀ (Fuc) ₄ (NH ₂ ·TFA) ₅ (subunits 12, 9, and 13)	2.4 (16.2)	52 \pm 13.3 (5.5)	>150 (1013.8)
tobramycin	2 (0.94)	92 \pm 9.4 (2.73)	2 (0.94)

^aEach value is the mean of at least three independent experiments that comprised six replicates at each concentration. ^bMBIC₅₀ = minimal biofilm inhibition concentration at which at least 50% reduction in biofilm formation was observed compared to the untreated control, determined by crystal violet assay. ^cMIC = minimal inhibitory concentration for bacterial growth. SD = standard deviation. SEM = standard error of mean. n.a. = not applicable.

galactosylated pillararene 1 promotes biofilm formation (Figure 2a) at high concentrations (>75 μ M). Such biofilm-promoting behavior had already been observed with glycopeptides.^{8c} Vidal et al. had also shown the ability of glycoclusters to aggregate the lectins LecA and LecB.^{18g} Furthermore, the comparison of molecules 4–6 shows that their antibiofilm activity is only moderately affected by the length and structure of the central axle of the rotaxanes (the only structural difference between molecules 4–6).

To further assess the structural determinants required for inhibiting biofilm formation, we compared the antibiofilm activity of rotaxane 6 to its isolated subunits (the central deacetylated deca-galactosylated pillar core 20, the deacetylated tetra-fucosylated thread 12, and the Boc-protected polyguanidinium subunit 13). Clearly, rotaxane 6 had significantly higher activity than all of its subcomponents at the same concentrations (Figure 2b). Moreover, the potency subunit 13 inhibited biofilm at MBIC₅₀ of 37.5 μ M while compounds 20 and 12 did not show any inhibitory activity (MBIC₅₀ > 150 μ M). This demonstrates that the synergistic effect of the three structural subunits of rotaxane 6 was important for the observed activity and that the polycationic module played an essential role in the antibiofilm activity.

Importantly, inspection of the MIC values by recording the absorbance (OD_{590nm} and OD_{600nm}) of molecules 1–6 at 590 and 600 nm (Table 2) shows that none of these heteroglycoclusters (neutral or polycationic) displays a bactericidal effect which demonstrates that inhibition of biofilm formation by rotaxanes 4–6 did not originate from an antibacterial activity (Figures S8 and S9, SI). Growth of planktonic cells was assessed by measuring OD at 590 nm every 30 min for 24 h (Figures S10–S12, SI); using this approach, no effect on growth could be observed for compounds 6 and 2, not even at the highest tested concentration (150 μ M). Tobramycin was used as a control molecule as this antibiotic shows strong antibiofilm activity via

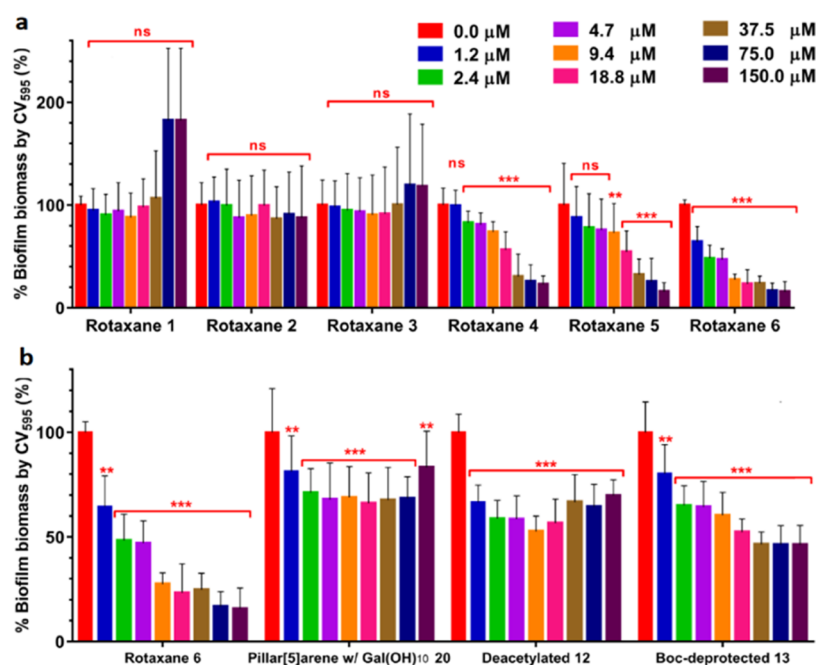


Figure 2. Inhibition of *P. aeruginosa* PAO1 biofilms. (a) Inhibition by heteroglyco[2]rotaxanes 1–6. Statistical significance was calculated using unpaired *t* test with Welch's correction and indicated by ****p* < 0.005 and ***p* < 0.05 compared with PBS-treated biofilms. ns: not significant. (b) Inhibition by heteroglyco[2]rotaxane 6 and its three structural subunits 13, 12, and 20. Data are presented as mean \pm SD. Statistical significance was calculated using unpaired *t* test with Welch's correction and indicated by ****p* < 0.001 and ***p* < 0.01 compared with PBS-treated biofilms.

a bactericidal mechanism (MBIC₅₀ = MIC; also see Figure S13, SI). Noteworthy, the level of *P. aeruginosa* antibiofilm activity of glycorotaxane 6 (MBIC₅₀ = 2.4 μ M) has rarely been reached in the literature for nonbactericidal molecules. To the best of our knowledge, the only comparable activity has been described by Reymond et al. for an optimized glycopeptide.^{8c} All other glycosylated *P. aeruginosa* biofilm inhibitors displayed either significantly lower potencies or comparable potencies combined with bactericidal activities.^{13,18}

Subsequently, the ability of rotaxanes 4–6 to disperse already established *P. aeruginosa* biofilms was evaluated by preincubating the bacteria under biofilm forming conditions for 24 h, followed by addition of compounds 4–6 at a concentration of 2.4 μ M, further incubation for another 24 h, and quantification of the residual biofilm as above. Percentages of biofilm eradication compared to untreated controls were similar for the three rotaxanes (30% for 4, 35% for 5 and 38% for 6 at a concentration of 2.4 μ M; Figure S14, SI), once again showing that the length of the central axle has only a moderate effect on the antibiofilm activity, which corroborates the results obtained by ITC.

To unambiguously demonstrate that lectins LecA and LecB are indeed the key targets at the origin of the antibiofilm activity of glycorotaxanes 4–6, we used a double Δ lecA Δ lecB mutant that we compared to the corresponding wild-type (WT) PAO1 strain (Figure S15, SI). Crystal violet assays were carried out in parallel with the two strains using the most active glycorotaxane 6 at three different concentrations (1.2, 18.8, and 150 μ M). At the highest concentration, a significant decrease in biofilm formation was observed with the wild type, whereas the level of biofilm formation was unaffected for the double mutant compared to a control. This experiment clearly shows that the antibiofilm activity of glycorotaxane 6 is lectin-dependent. To strengthen this conclusion, we performed an antibiofilm assay with molecules 6 and 2 against *Staphylococcus*

aureus Mu50, a Gram-positive bacterium that does not express LecA and LecB. As expected, no antibiofilm activity was observed (Figure S16, SI).

Mammalian Cell Toxicity and Human Red Blood Cell Hemolysis Assays. Finally, the toxicity of molecules 4–6 toward eukaryotic cells was evaluated using two distinct assays. Primarily, standard cytotoxicity MTT assay on human A549 lung cells showed that none of the rotaxanes 4–6 were cytotoxic at concentrations up to 250 μ M (Figures S17 and S18, SI). Next, given the potential of polycationic peptides and amphiphiles to disrupt mammalian cell membranes, we measured the hemolytic activity of rotaxanes 4–6 on human red blood cells (Figures S19 and S20, SI). Likewise, none of the rotaxanes 4–6 exhibited hemolytic activities at concentrations up to 75 μ M, well above their MBIC₅₀ values.

CONCLUSIONS

In summary, a series of novel heterovalent glyco[2]rotaxanes were efficiently prepared thanks to the supramolecular assembly of a central deca-galactosylated pillar[5]arene, a tetra-fucosylated dendron, and a polyguanidinium tail. ITC analyses showed that the binding affinities of each heteroglycorotaxane toward the two targeted bacterial lectins LecA and LecB of *P. aeruginosa* were high and not affected by the polycationic tail. The inhibition assays of *P. aeruginosa* biofilm growth demonstrated that: (1) the three noncationic rotaxanes 1–3 bearing the two lectins ligands do not display significant antibiofilm activities, (2) the best rotaxane 6 showed a level of antibiofilm activity (MBIC₅₀ = 2.4 μ M) rarely reached in the literature, (3) the three subunits of the rotaxanes 4–6 (the two glycosylated selectivity modules and the polycationic potency module) synergistically cooperate and participate to the global antibiofilm activity, and (4) the antibiofilm activity is lectin-dependent as demonstrated by the lack of antibiofilm activity of the most active molecules on a Δ lecA Δ lecB *P. aeruginosa*

mutant. Probably the most remarkable feature of glycorotaxanes 4–6 is the absence of any bactericidal effect, which means that their ability to prevent biofilm formation is not linked to the eradication of the bacteria themselves. Having now in hand all of the elements and parameters required for efficient antibiofilm activity, our next objective will be to design a second generation of molecules with a simpler structure.

As a direct perspective, we may also envision the design of glycorotaxanes inhibiting both the biofilm formation and the adhesion of bacteria to their host cells. Indeed, homo- and heteroglycoclusters have also been explored as antiadhesive molecules for various pathogens,^{17a,26} including *P. aeruginosa*.^{18g,27} Our present work thus opens the way to molecules presenting dual antiadhesive and antibiofilm activities. In line with the objectives of the present study, research efforts have been made to produce functional materials incorporating bactericidal elements that could also help to develop efficient antibiofilm agents.²⁸

■ EXPERIMENTAL SECTION

General Conditions. Chemicals, unless otherwise stated, were obtained from commercial sources. Solvents were all of commercial grade and employed as purchased. Dry diethyl ether (Et₂O), tetrahydrofuran (THF), and dichloromethane (CH₂Cl₂) were taken from PureSolv Micro solvent purification system. Solvents used for column chromatography including ethyl acetate (EtOAc), cyclohexane, and CH₂Cl₂ were purchased in industrial grade and further distilled before use. Acetonitrile (MeCN) and pyridine were dried prior to their use by the usual distillation over CaH₂ under argon (Ar). Deuterated solvents (CDCl₃, D₂O, CD₃OD, and (CD₃)₂SO) for NMR analysis were purchased from Cambridge Isotopes Laboratories (Eurisotop). All reactions were carried out in standard glassware under an argon atmosphere (Ar) with anhydrous solvents, unless otherwise noted. Evaporation and concentration were done at water aspirator pressure (rotary evaporator) and drying in vacuo at 10–2 Torr. Degassing (sparging) of solvents, when needed, was performed by bubbling argon gas for 10–15 min. Reactions were monitored by thin-layer chromatography (TLC) on aluminum sheets coated with silica gel 60 F₂₅₄ (0.25 mm, E. Merck), and spots were visualized by ultraviolet light ($\lambda = 254$ nm, 365 nm) and/or by staining with ninhydrin in ethanol solution or charring with a yellow solution of phosphomolybdic acid (PMA) [(NH₄)Mo₇O₂₄·4H₂O (120 g) and (NH₄)₂Ce(NO₃)₆ (5 g) in 10% H₂SO₄ (800 mL)] or a purple solution of potassium permanganate [KMnO₄ (1.5 g), K₂CO₃ (10 g), and 10% NaOH (1.25 mL) in water (200 mL)]. Chromatographic separations were performed on a silica gel (Kiesel gel 60, 230–400 mesh, 0.040–0.063 mm, E. Merck) column by flash chromatography. Compounds were confirmed to have >95% purity. NMR experiments were performed in deuterated solvents. 1D NMR (¹H, ¹³C, DEPT) spectra were recorded on a JEOL (ECX-400 or ECX-500) spectrometer at 400 and 500 MHz for proton resonance and at 101 and 126 MHz for carbon resonance. Two-dimensional (2D) NMR spectra were recorded on a JEOL (ECX-500) spectrometer. ¹H chemical shifts were reported (in ppm) referred to the deuterated solvent used for the sampling (7.26 for CDCl₃-d₁, 4.79 for D₂O-d₂, 3.31 for CD₃OD-d₄, and 2.50 for ((CD₃)₂SO-d₆). ¹³C chemical shifts were reported (in ppm) relative to the residual solvent signal (77.16 for CDCl₃, 49.00 for CD₃OD-d₄, and 39.52 for (CD₃)₂SO-d₆). ¹H NMR spectral data features are tabulated in the following order: chemical shift (δ) in ppm (multiplicity, coupling constant (*J*), integration, label/type of H). The following abbreviations were used to label the multiplicities in the NMR data: s = singlet, br = broad, app = apparent, d = doublet, t = triplet, q = quartet, pent = pentet, quint = quintet, appd = apparent doublet, appq = apparent quartet, dd = doublet of doublets, m = multiplet, br s = broad singlet and 2 s = two singlets. Assignment of signals in ¹H and ¹³C NMR were performed using 2D ¹H–¹H COSY, HMQC, HSQC, HMBC, and

DEPT135 (dept polarization transfer with 135° read pulse to give XH, XH₃ positive, and XH₂ negative with decoupling during acquisition) experiments where appropriate. IR spectra were recorded on a PerkinElmer RX 1 FT-IR spectrometer Frontier with frequencies expressed in cm⁻¹. Subtraction of the background was performed before recording the spectra. Liquid and solid samples were directly placed on the surface of the central diamond crystal. Optical activities of chiral molecules were measured on a PerkinElmer 241 spectrometer using a sodium lamp ($\lambda = 589$ nm) at room temperature. Positive-ion matrix-assisted LASER desorption/ionization-mass spectrometry (MALDI-TOF-MS) analyses for sample 2a were performed using a Waters QTOF Premier mass spectrometer equipped with a Nd:YAG laser operating at 355 nm (third harmonic) with a maximum output of 65 μ J delivered to the sample in 2.2 ns pulses at a 50 Hz repeating rate. Time-of-flight mass analysis was performed in the reflectron mode at a resolution of about 10k (*m/z* 569). All samples were analyzed using trans-2-[3-(4-*tert*-butylphenyl)-2-methylprop-2-enylidene]malononitrile (DCTB) as a matrix. Rotaxane samples were solubilized in acetonitrile to obtain 1 mg·mL⁻¹ solution. Additionally, 40 μ L of 2 mg·mL⁻¹ NaI solution in acetonitrile was added to the rotaxane solution. ESI-MS measurements were performed either on a Waters Synapt G2-Si mass spectrometer (UK) equipped with an Electrospray ionization source used in the positive-ion mode (molecules 4a, 2c, 3b, and 3c) or on a Bruker maXis Impact HD Q-TOF spectrometer in positive mode (rest of molecules).

Isothermal titration calorimetry (ITC) was performed with a VP-ITC isothermal titration calorimeter (MicroCal-Malvern) and protein concentration was checked using Nanodrop 2000 UV–vis spectrophotometer ($\lambda = 280$ nm).

Bacterial optical density (0.2 at 600 nm) was measured on a Thermo Scientific spectrophotometer. Measurements of the optical density (OD₆₀₀) and absorbance ($\lambda = 595$ nm) in the biofilm inhibition and dispersal assays were recorded using a Tecan plate reader SpectraMax iD3-Multimode Microplate Reader.

Toxicity to human cells was evaluated by MTT (3-[4,5-dimethylthiazoyl-2-yl]-2,5-diphenyl tetrazolium bromide) assay. The absorbance was read at OD = 570 nm using a plate reader xMark Microplate Absorbance Spectrophotometer (Bio-Rad).

In human red blood cell hemolysis assay, the absorbance was read at OD = 540 nm using a microplate reader SpectraMax-M2.

Gram-negative *Pseudomonas aeruginosa* bacterial PAO1 strain was offered by Prof. Dr. Tom Coenye (Laboratory of Pharmaceutical Microbiology, Ghent University, Belgium). Bacteria initially received on a Petri dish containing Tryptic Soy Broth (TSB) were incubated for 24 h at 37 °C. Next, few bacterial colonies were taken and dispersed in the Cryobank tubes containing the preservation medium and color-coded ceramic beads. These tubes were then centrifuged at 2000–3000 rpm and the maximum amount of glycerol broth was removed before freezing them at –80 °C. For biological assays, bacteria were streaked from these –80 °C glycerol stocks on Tryptic Soy Broth (TSB). All experiments were conducted at 37 °C. All glassware used in this study were sterilized before test.

Tetra- α -fucosidic Alkyne Linker (10). To a solution of tetra- α -fucosidic TMS-protected alkyne 10a (1.0 equiv, 0.371 mmol, 0.85 g) in dry THF (13.5 mL) at 0 °C was added TBAF·3H₂O (1.2 equiv, 0.441 mmol, 0.117 g). The solution was stirred for 5 min at 0 °C. Afterward, the solvent was removed by rotary evaporation under vacuum, and the resulting residue was dissolved in CH₂Cl₂ (15 mL), washed with a saturated aqueous solution of NH₄Cl (2 \times 10 mL) and brine (1 \times 10 mL), dried over MgSO₄, filtered, and concentrated again under vacuum. The crude was purified by column chromatography on silica gel (SiO₂) using a gradient eluent of EtOAc (100%) then EtOAc/MeOH (80:20 to 90:10) to give compound 10 as a fluffy shiny off-white solid (0.367 mmol, 0.816 g, 99%). Purity is >95%. This product is hygroscopic, if left open to air, it turns to a gel. *R*_f = 0.23 in pentane/EtOAc (90:10). ¹H NMR (500 MHz, CDCl₃-d₁): δ _H = 7.78 (br s, 1H, CH, H-16), 7.72 (br s, 1H, CH, H-16'), 7.68 (br s, 2H, 2 \times CH, H-11), 7.66 (br s, 2H, 2 \times CH, H-11'), 7.56 (d, *J* = 8.2 Hz, 2H, 2 \times CH_{Ar}, H-21), 7.46 (d, *J* = 8.3 Hz, 2H, 2 \times CH_{Ar}, H-22),

5.27 (dd, $J = 9.9, 3.3$ Hz, 4H, $4 \times \text{CH}$, H-3), 5.22–5.21 (m, 4H, $4 \times \text{CH}$, H-4), 5.06–5.03 (m, 8H, $8 \times \text{CH}$, H-1, H-2), 4.89 (pent, $J = 5.3$ Hz, 2H, $2 \times \text{CH}$, H-15), 4.58 (br s, 10H, $5 \times \text{CH}_2$, H-13, H-18), 4.47 (br s, 10H, $5 \times \text{CH}_2$, H-10, H-18'), 4.07 (q, $J = 5.5$ Hz, 4H, $4 \times \text{CH}$, H-5), 3.94–3.91 (m, 8H, $4 \times \text{CH}_2$, H-14), 3.82 (t, $J = 4.6$ Hz, 8H, $4 \times \text{CH}_2$, H-9), 3.71 (dd, $J = 7.7, 5.9$ Hz, 4H, $4 \times \text{CH}$ -a, H-7a), 3.56–3.54 (m, 12H, $4 \times \text{CH}$ -b and $4 \times \text{CH}_2$, H-8, H-7b), 3.12 (s, 1H, CH, H-25), 2.11 (s, 12H, $4 \times \text{CH}_3$, OCOCH₃), 1.99 (s, 12H, $4 \times \text{CH}_3$, OCOCH₃), 1.93 (s, 12H, $4 \times \text{CH}_3$, OCOCH₃), 1.06 (dd, $J = 6.5, 1.9$ Hz, 12H, $4 \times \text{CH}_3$, H-6). ¹³C NMR (126 MHz, CDCl₃-d₁): $\delta_{\text{C}} = 170.8$ (Cq, C-19), 170.5 ($4 \times \text{Cq}$, C=O), 170.3 ($4 \times \text{Cq}$, C=O), 170.0 ($4 \times \text{Cq}$, C=O), 144.0 ($4 \times \text{C}_{\text{triazole}}$, C-12), 143.1 (Cq_{triazole}, C-17), 142.3 (Cq_{triazole}, C-17'), 135.8 (Cq_{Ar}, C-20), 132.1 ($2 \times \text{CH}_{\text{Ar}}$, C-22), 127.5 ($2 \times \text{CH}_{\text{Ar}}$, C-21), 123.8 ($4 \times \text{CH}$, C-11), 123.6 (Cq_{Ar}, C-23), 123.3 ($2 \times \text{CH}$, C-16), 96.1 ($4 \times \text{CH}$, C-1), 82.8 (CH, C-25), 78.9 (Cq, C-24), 70.9 ($4 \times \text{CH}$, C-4), 70.1 ($4 \times \text{CH}_2$, C-8), 69.3 ($4 \times \text{CH}_2$, C-9), 68.7 ($4 \times \text{CH}_2$, C-14), 68.0 ($4 \times \text{CH}$, C-2), 67.8 ($4 \times \text{CH}$, C-3), 67.14 ($4 \times \text{CH}_2$, C-7), 64.4 ($2 \times \text{CH}_2$, C-13), 64.35 ($2 \times \text{CH}_2$, C-13'), 64.3 ($4 \times \text{CH}$, C-5), 60.5 ($2 \times \text{CH}$, C-15), 50.1 ($4 \times \text{CH}_2$, C-10), 44.0 (CH₂, C-18), 39.5 (CH₂, C-18'), 20.8 ($4 \times \text{CH}_3$, OCOCH₃), 20.7 ($4 \times \text{CH}_3$, OCOCH₃), 20.6 ($4 \times \text{CH}_3$, OCOCH₃), 15.8 ($4 \times \text{CH}_3$, C-6). IR (neat): $U_{\text{max}}/\text{cm}^{-1}$ 3276 (C-H alkyne), 2210 (C≡C). HRMS (ESI-TOF) (m/z): [M + H]⁺ Calcd for C₉₇H₁₃₄N₁₉O₄₁: 2220.9017, requires 2220.8979.

General Procedure for the Synthesis of 11 and 12. To a solution of tetra- α -fucosidic alkyne **10** (1.0 equiv, 0.18 mmol, 0.4 g) and diazidoalkanes **7** or **8** (3.0 equiv, 0.54 mmol) in dry CHCl₃ (2 mL) was added CuBr-SMe₂ (2.0 equiv, 0.36 mmol, 0.074 g), and the mixture was stirred at room temperature for 12 h. The solution was diluted with CH₂Cl₂ (15 mL) and washed with a saturated aqueous solution of NH₄Cl (2 \times 10 mL). The aqueous phase was extracted with CH₂Cl₂ (3 \times 15 mL), and the organic phase was dried over MgSO₄, filtered, and concentrated by rotary evaporation under reduced pressure. The residue was purified by column chromatography on silica gel (SiO₂) using EtOAc/MeOH to afford the desired threads **11** and **12**.

Tetra- α -fucosidic [2]rotaxane Thread (11). The title compound was prepared using tetra- α -fucosidic alkyne **10** and 1,10-diazidodecane **7** (0.122 g) according to general procedure, purified by column chromatography on silica gel (SiO₂) using EtOAc (100%) then EtOAc/MeOH (90:10), and isolated as a pale yellow fluffy shiny solid (0.16 mmol, 0.392 g, 89%). Purity is >95%. $R_f = 0.33$ in pentane/EtOAc (80:20). ¹H NMR (500 MHz, CDCl₃-d₁): $\delta_{\text{H}} = 7.80$ (br s, 1H, CH, H-16), 7.71 (d, $J = 7.5$ Hz, 3H, CH and $2 \times \text{CH}_{\text{Ar}}$, H-25, H-22), 7.62–7.61 (m, 5H, $5 \times \text{CH}$, H-11, H-16'), 7.52 (d, $J = 7.4$ Hz, 2H, $2 \times \text{CH}_{\text{Ar}}$, H-21), 5.17 (d, $J = 10.5$ Hz, 4H, $4 \times \text{CH}$, H-3), 5.12 (br s, 4H, $4 \times \text{CH}$, H-4), 4.95–4.94 (m, 8H, $8 \times \text{CH}$, H-1, H-2), 4.89 (pent, $J = 5.3$ Hz, 2H, $2 \times \text{CH}$, H-15), 4.60 (br s, 2H, CH₂, H-18), 4.50 (br s, 8H, $4 \times \text{CH}_2$, H-13), 4.46 (br s, 2H, CH₂, H-18'), 4.39 (br s, 8H, $4 \times \text{CH}_2$, H-10), 4.28 (t, $J = 6.6$ Hz, CH₂, H-26), 3.98 (app q, $J = 3.9$ Hz, 4H, $4 \times \text{CH}$, H-5), 3.84 (d, $J = 6.1$ Hz, 8H, $4 \times \text{CH}_2$, H-14), 3.73 (br s, 8H, $4 \times \text{CH}_2$, H-9), 3.62–3.60 (m, 4H, $4 \times \text{CH}$ -a, H-7a), 3.47–3.45 (m, 12H, $4 \times \text{CH}$ -b and $4 \times \text{CH}_2$, H-7b, H-8), 3.11 (t, $J = 6.8$ Hz, 2H, CH₂, H-35), 2.02 (s, 12H, $4 \times \text{CH}_3$, OCOCH₃), 1.89 (s, 12H, $4 \times \text{CH}_3$, OCOCH₃), 1.84 (s, 12H, $4 \times \text{CH}_3$, OCOCH₃), 1.45–1.43 (m, 2H, CH₂, H-34), 1.21–1.15 (m, 14H, $7 \times \text{CH}_2$, H-27 to H-33), 0.97 (d, $J = 6.0$ Hz, 12H, $4 \times \text{CH}_3$, H-6). ¹³C NMR (126 MHz, CDCl₃-d₁): $\delta_{\text{C}} = 171.1$ (Cq, C-19), 170.4 ($4 \times \text{Cq}$, C=O), 170.2 ($4 \times \text{Cq}$, C=O), 169.8 ($4 \times \text{Cq}$, C=O), 146.5 (Cq_{triazole}, C-24), 143.9 ($4 \times \text{C}_{\text{triazole}}$, C-12), 143.0 (Cq_{triazole}, C-17), 142.5 (Cq_{triazole}, C-17'), 134.8 (Cq_{Ar}, C-23), 132.1 (Cq_{Ar}, C-20), 127.9 ($2 \times \text{CH}_{\text{Ar}}$, C-21), 125.3 ($2 \times \text{CH}_{\text{Ar}}$, C-22), 123.7 ($4 \times \text{CH}$, C-11), 123.5 (CH, C-16), 123.0 (CH, C-16'), 120.1 (CH, C-25), 96.0 ($4 \times \text{CH}$, C-1), 70.8 ($4 \times \text{CH}$, C-4), 69.9 ($4 \times \text{CH}_2$, C-8), 69.2 ($4 \times \text{CH}_2$, C-9), 68.6 ($4 \times \text{CH}_2$, C-14), 67.9 ($4 \times \text{CH}$, C-2), 67.6 ($4 \times \text{CH}$, C-3), 67.0 ($4 \times \text{CH}_2$, C-7), 64.3 ($4 \times \text{CH}_2$, C-13), 64.1 ($4 \times \text{CH}$, C-5), 60.3 ($2 \times \text{CH}$, C-15), 51.2 (CH₂, C-35), 50.2 (CH₂, C-26), 49.96 ($4 \times \text{CH}_2$, C-10), 44.1 (CH₂, C-18), 39.6 (CH₂, C-18'), 30.1 (CH₂, C-34), 29.1 (CH₂, C-30), 29.0 (CH₂, C-31), 28.8 (CH₂, C-29), 28.7 (CH₂, C-32), 28.5 (CH₂, C-27), 26.4 (CH₂, C-28), 26.2 (CH₂, C-33), 20.6 (4

$\times \text{CH}_3$, OCOCH₃), 20.5 ($4 \times \text{CH}_3$, OCOCH₃), 20.44 ($4 \times \text{CH}_3$, OCOCH₃), 15.6 ($4 \times \text{CH}_3$, C-6). IR (neat): $U_{\text{max}}/\text{cm}^{-1}$ 2095 (N₃). HRMS (ESI-TOF) (m/z): [M + 2H]²⁺ Calcd for C₁₀₇H₁₅₅N₂₅O₄₁: 1223.0401, requires 1223.0397.

Tetra- α -fucosidic [2]Rotaxane Thread (12). The title compound was prepared using tetra- α -fucosidic alkyne **10** and 1,12-diazidodecane **8** (0.136 g) according to general procedure **D**, purified by column chromatography on silica gel (SiO₂) using EtOAc (100%) then EtOAc/MeOH (90:10), and isolated as a pale yellow fluffy shiny solid (0.138 mmol, 0.341 g, 77%). Purity is >95%. $R_f = 0.11$ in pentane/EtOAc (90:10). ¹H NMR (500 MHz, CDCl₃-d₁): $\delta_{\text{H}} = 7.81$ (br s, 1H, CH, H-16), 7.75 (d, $J = 8.1$ Hz, 3H, CH and $2 \times \text{CH}_{\text{Ar}}$, H-25, H-22), 7.66–7.64 (m, 5H, $5 \times \text{CH}$, H-11, H-16'), 7.54 (d, $J = 8.2$ Hz, 2H, $2 \times \text{CH}_{\text{Ar}}$, H-21), 5.21 (dd, $J = 9.8, 3.2$ Hz, 4H, $4 \times \text{CH}$, H-3), 5.16 (d, $J = 2.0$ Hz, 4H, $4 \times \text{CH}$, H-4), 5.02–4.93 (m, 8H, $8 \times \text{CH}$, H-1, H-2), 4.85 (pent, $J = 5.5$ Hz, 2H, $2 \times \text{CH}$, H-15), 4.6 (br s, 2H, CH₂, H-18), 4.54 (br s, 8H, $4 \times \text{CH}_2$, H-13), 4.49 (br s, 2H, CH₂, H-18'), 4.43–4.41 (m, 8H, $4 \times \text{CH}_2$, H-10), 4.31 (t, $J = 7.2$ Hz, CH₂, H-26), 4.04–4.00 (m, 4H, $4 \times \text{CH}$, H-5), 3.90–3.83 (m, 8H, $4 \times \text{CH}_2$, H-14), 3.77 (t, $J = 5.1$ Hz, 8H, $4 \times \text{CH}_2$, H-9), 3.68–3.62 (m, 4H, $4 \times \text{CH}$ -a, H-7a), 3.52–3.49 (m, 12H, $4 \times \text{CH}$ -b and $4 \times \text{CH}_2$, H-7b, H-8), 3.15 (t, $J = 7.0$ Hz, 2H, CH₂, H-37), 2.06 (s, 12H, $4 \times \text{CH}_3$, OCOCH₃), 1.93 (s, 12H, $4 \times \text{CH}_3$, OCOCH₃), 1.89 (s, 12H, $4 \times \text{CH}_3$, OCOCH₃), 1.48 (pent, $J = 7.5$ Hz, 2H, CH₂, H-36), 1.30–1.13 (m, 18H, $9 \times \text{CH}_2$, H-27 to H-35), 1.00 (dd, $J = 6.4, 1.6$ Hz, 12H, $4 \times \text{CH}_3$, H-6). ¹³C NMR (126 MHz, CDCl₃-d₁): $\delta_{\text{C}} = 171.3$ (Cq, C-19), 170.4 ($4 \times \text{Cq}$, C=O), 170.2 ($4 \times \text{Cq}$, C=O), 169.9 ($4 \times \text{Cq}$, C=O), 146.6 (Cq_{triazole}, C-24), 144.0 ($4 \times \text{C}_{\text{triazole}}$, C-12), 143.2 (Cq_{triazole}, C-17), 142.6 (Cq_{triazole}, C-17'), 135.0 (Cq_{Ar}, C-23), 132.2 (Cq_{Ar}, C-20), 128.0 ($2 \times \text{CH}_{\text{Ar}}$, C-21), 125.4 ($2 \times \text{CH}_{\text{Ar}}$, C-22), 123.8 ($4 \times \text{CH}$, C-11), 123.6 (CH, C-16), 123.1 (CH, C-16'), 120.1 (CH, C-25), 96.1 ($4 \times \text{CH}$, C-1), 70.9 ($4 \times \text{CH}$, C-4), 70.1 ($4 \times \text{CH}_2$, C-8), 69.3 ($4 \times \text{CH}_2$, C-9), 68.8 ($4 \times \text{CH}_2$, C-14), 68.0 ($4 \times \text{CH}$, C-2), 67.8 ($4 \times \text{CH}$, C-3), 67.1 ($4 \times \text{CH}_2$, C-7), 64.4 ($4 \times \text{CH}_2$, C-13), 64.2 ($4 \times \text{CH}$, C-5), 60.4 ($2 \times \text{CH}$, C-15), 51.3 (CH₂, C-37), 50.3 (CH₂, C-26), 50.1 ($4 \times \text{CH}_2$, C-10), 44.2 (CH₂, C-18), 39.8 (CH₂, C-18'), 30.2 (CH₂, C-36), 29.3 (CH₂-axle), 29.27 (CH₂-axle), 29.26 (CH₂-axle), 29.2 (CH₂-axle), 29.0 (CH₂-axle), 28.8 (CH₂-axle), 28.7 (CH₂-axle), 26.5 (CH₂-axle), 26.3 (CH₂-axle), 20.7 ($4 \times \text{CH}_3$, OCOCH₃), 20.6 ($4 \times \text{CH}_3$, OCOCH₃), 20.5 ($4 \times \text{CH}_3$, OCOCH₃), 15.7 ($4 \times \text{CH}_3$, C-6). IR (neat): $U_{\text{max}}/\text{cm}^{-1}$ 2097 (N₃). HRMS (ESI-TOF) (m/z): [M + 2H]²⁺ Calcd for C₁₀₉H₁₅₉N₂₅O₄₁: 1237.0557, requires 1237.5581.

Clickable N-Boc-Protected Tetrapeptide (13). To a stirred solution of **17** (1.0 equiv, 0.182 mmol, 0.291 g) in dry CH₂Cl₂ (7.1 mL) were added propargyl amine (2.4 equiv, 0.438 mmol, 0.029 mL) and HOBt (1.3 equiv, 0.237 mmol, 0.032 g) under an argon atmosphere. The reaction mixture was cooled down to 0 °C before adding EDCI (2.0 equiv, 0.364 mmol, 0.07 g) and stirring was continued overnight (16 h) during which the temperature increased slowly to room temperature. Next, the resulting solution was treated with a saturated aqueous solution of NaHCO₃ (2 \times 10 mL) and extracted with CH₂Cl₂ (2 \times 20 mL). The organic layers were combined, washed with H₂O (10 mL) and brine (2 \times 10 mL), dried over MgSO₄, and concentrated by rotary evaporation under reduced pressure. The brown residue was purified by column chromatography on silica gel (SiO₂) using CH₂Cl₂/MeOH (99:1 to 98:2) as a gradient eluent to furnish the desired clickable tetrapeptide **13** as a colorless shiny solid (0.12 mmol, 0.2 g, 67%). Purity is >95%. $R_f = 0.11$ in CH₂Cl₂/MeOH (98:2). ¹H NMR (500 MHz, CDCl₃-d₁): $\delta_{\text{H}} = 11.42$ (br s, 4H, NHBoc, 8.30–8.26 (m, 4H, NH-C=NBoc), 7.32 (br s, 1H, NH), 7.22 (br s, 1H, NH), 7.10–6.99 (m, 1H, NH), 6.64 (br s, 1H, NH), 5.56, 5.35 (2 s, 1H, NH), 4.34 (br s, 1H, CH, H-1'), 4.24 (br s, 1H, CH, H-1''), 4.15 (br s, 1H, CH, H-1'''), 4.04–4.01 (m, 1H, CH₂a, H-14a), 3.92–3.89 (m, 1H, CH₂b, H-14b), 3.82 (br s, 1H, CH, H-1), 3.36 (br s, 8H, $4 \times \text{CH}_2$, H-5), 2.29, 2.22 (2 s, 1H, CH, H-16), 1.70–1.41 (m, 105H, 27 \times CH₂ and 12 \times CH₂, H-8, H-8', H-2, H-3, H-4). ¹³C NMR (126 MHz, CDCl₃-d₁): $\delta_{\text{C}} = 173.5, 172.4, 171.8, 171.6$ ($4 \times \text{Cq}$, C-13, C-6, C-6'), 163.5, 163.44, 163.42, 163.4 ($4 \times \text{Cq}$, C-10), 157.0 (Cq, C-7), 156.5, 156.2, 156.1, 156.0 ($4 \times \text{Cq}$, C-11), 153.21,

153.2, 153.1 (4 × Cq, C-12), 83.1, 83.0, 82.98, 82.97 (4 × Cq, C-8'), 81.3, 80.4 (Cq, C-8), 79.7, 79.6 (CH, C-16), 79.3, 79.21, 79.12, 79.1 (4 × Cq, C-8''), 71.7, 71.2 (Cq, C-15), 56.6 (CH, C-1''), 55.0, 54.6, 54.5, 53.8, 53.5, 52.7 (3 × CH, C-1, C-1'), 40.8, 40.6, 40.53, 40.5, 40.4, 40.2 (4 × CH₂, C-5), 31.2, 31.08, 31.06, 30.9 (4 × CH₂, C-2), 29.11, 29.1 (CH₂, C-14), 28.8, 28.7 (4 × CH₂, C-4), 28.3, 28.25, 28.2, 28.0 (27 × CH₃, C-9, C-9', C-9''), 23.8, 23.5, 23.4, 23.2, 23.1, 23.0 (4 × CH₂, C-3). HRMS (ESI-TOF) (*m/z*): [M + 2H]²⁺ Calcd for C₇₆H₁₃₃N₁₇O₂₂: 818.9961, requires 818.9978.

Clickable N-Boc-Protected Tetrapeptide (14). To a stirred solution of **17** (1.0 equiv, 0.186 mmol, 0.298 g) in dry CH₂Cl₂ (7.2 mL) were added hex-5-yn-1-amine (2.4 equiv, 0.446 mmol, 0.054 mL) and HOBt (1.3 equiv, 0.242 mmol, 0.033 g) under an argon atmosphere. The reaction mixture was cooled down to 0 °C before adding EDCI (2.0 equiv, 0.372 mmol, 0.071 g) and stirring was continued overnight (16 h) during which the temperature increased slowly to room temperature. Next, the resulting solution was treated with a saturated aqueous solution of NaHCO₃ (2 × 10 mL) and extracted with CH₂Cl₂ (2 × 20 mL). The organic layers were combined, washed with H₂O (10 mL) and brine (2 × 10 mL), dried over MgSO₄, and concentrated by rotary evaporation under reduced pressure. The orange residue was purified by column chromatography on silica gel (SiO₂) using CH₂Cl₂/MeOH (99:1 to 98:2) as a gradient eluent to furnish the desired clickable tetrapeptide **14** as a colorless shiny solid (0.15 mmol, 0.251 g, 81%). Purity is >95%. *R*_f = 0.15 in CH₂Cl₂/MeOH (98:2). ¹H NMR (500 MHz, CDCl₃-d₁): δ_H = 11.37–11.36 (m, 4H, *NHBoc*), 8.21–8.17 (m, 4H, *NH-C=NBoc*), 7.29 (br s, 1H, NH), 7.09 (br s, 1H, NH), 6.72 (br s, 2H, 2 × NH), 5.62 (br s, 1H, NH), 4.18 (br s, 1H, CH, H-1'), 4.10 (br s, 1H, CH, H-1''), 3.99 (br s, 1H, CH, H-1'''), 3.68 (br s, 1H, CH, H-1), 3.32–3.26 (m, 8H, 4 × CH₂, H-5), 3.20–3.14 (m, 1H, CH₂a, H-14a), 3.08–3.05 (m, 1H, CH₂b, H-14b), 2.08–2.05 (m, 2H, CH₂, H-17), 1.89, 1.86 (2 t, *J* = 2.0 Hz, 1H, CH, H-19), 1.65–1.33 (m, 109H, 27 × CH₃ and 14 × CH₂, H-8, H-8', H-2, H-3, H-4, H-15, H-16). ¹³C NMR (126 MHz, CDCl₃-d₁): δ_C = 173.8, 172.6, 171.7 (4 × Cq, C-13, C-6, C-6'), 163.4, 163.3, 163.2 (4 × Cq, C-10), 157.1 (Cq, C-7), 156.0, 156.2, 155.95, 155.93, 155.86, 155.85, 155.8 (4 × Cq, C-11), 153.1, 153.01, 153.0 (4 × Cq, C-12), 84.2, 84.1 (CH, C-19), 83.0, 82.9, 82.84, 82.8 (4 × Cq, C-8'), 81.1, 80.2 (Cq, C-8), 79.1, 79.03, 79.0, 78.97, 78.9 (4 × Cq, C-8''), 63.7, 68.4 (Cq, C-18), 56.9 (CH, C-1'), 53.4, 54.8, 53.8 (3 × CH, C-1, C-1'), 40.7, 40.5, 40.3, 40.1 (4 × CH₂, C-5), 38.8, 38.7 (CH₂, C-14), 30.9, 30.87, 30.8 (4 × CH₂, C-2), 28.6, 28.5 (5 × CH₂, C-4, C-15), 28.2, 28.11, 28.1, 27.9 (27 × CH₃, C-9, C-9', C-9''), 25.5 (CH₂, C-16), 24.0, 23.6, 23.1, 22.9 (4 × CH₂, C-3), 17.9 (CH₂, C-17). HRMS (ESI-TOF) (*m/z*): [M + H]⁺ Calcd for C₇₉H₁₄₀N₁₇O₂₂: 1679.0356, requires 1679.0353.

General Procedure G for the Synthesis of 4c–6c. To a solution of **4b–6b** (1.0 equiv) and alkyne β-D-galactopyranoside **18** (12.0 equiv) kept under an argon atmosphere in CH₂Cl₂ (0.023 M) was added a freshly prepared solution of CuSO₄·5H₂O (0.5 equiv) and sodium ascorbate (1.5 equiv) in H₂O (0.022 M). The solution was degassed three times and stirred at room temperature for 24 h. The solution was concentrated by rotary evaporation under vacuum, redissolved in CH₂Cl₂ (10 mL), and washed with a saturated aqueous solution of NH₄Cl (3 × 5 mL). The aqueous phase was extracted with CH₂Cl₂ (2 × 10 mL) and the combined organic layers were washed with brine (1 × 10 mL), dried over MgSO₄, filtered, and concentrated under reduced pressure. The residue was purified by column chromatography on silica gel (SiO₂) using a gradient eluent of CH₂Cl₂ (100%) then CH₂Cl₂/MeOH (99:1 to 97:7) to afford the desired products **4c–6c**.

Deca-Galactosylated Hetero[2]rotaxane 4c. The title compound **4c** was prepared using **4b** (0.0084 mmol, 0.045 g), **18** (0.10 mmol, 0.039 g), CuSO₄·5H₂O (0.0042 mmol, 0.001 g), and sodium ascorbate (0.0126 mmol, 0.0025 g) in CH₂Cl₂/H₂O (0.37:0.19 mL) according to general procedure **G** and isolated as a yellow viscous gel that solidified to pale yellow glassy solid (0.0065 mmol, 0.060 g, 78%). Purity is >95%. *R*_f = 0.24 in CH₂Cl₂/MeOH (95:5). ¹H NMR (500 MHz, CDCl₃-d₁): δ_H = 11.40 (br s, 4H, *NHBoc*), 8.26–8.21 (m, 4H, *NH-C=NBoc*), 7.98–7.96 (m, 2H, 2 × CH_{Ar}, H-

22), 7.85–7.82 (m, 4H, 2 × CH and 2 × CH_{Ar}, H-16, H-16', H-21), 7.77–7.67 (m, 14H, 14 × CH, H-66, H-11), 7.54 (br s, 1H, CH, H-36), 7.48 (br s, 1H, CH, H-25), 7.42 (d, *J* = 6.4 Hz, 1H, NH), 7.33 (br s, 1H, NH), 7.16 (br s, 2H, NH), 6.67–6.66 (m, 10H, 10 × CH_{Ar}, H-58, H-61), 5.30 (br s, 10H, 10 × CH, H-72), 5.24 (br s, 4H, 4 × CH, H-3), 5.19 (br s, 4H, 4 × CH, H-4), 5.12–5.07 (m, 10H, 10 × CH, H-70), 5.02–5.00 (m, 8H, 8 × CH, H-1, H-2), 4.95–4.82 (m, 20H, 5 × CH₂ and 10 × CH, H-68, H-71), 4.82 (br s, 2H, 2 × CH, H-15), 4.73–4.67 (m, 30H, 15 × CH₂, H-64, H-68'), 4.61–4.58 (m, 10H, 10 × CH, H-69), 4.55 (br s, 12H, 6 × CH₂, H-13, H-18, H-18'), 4.46 (br s, 8H, 4 × CH₂, H-10), 4.27–4.16 (m, 23H, 3 × CH and 10 × CH₂, H-40, H-42, H-44, H-63, H-63'), 4.07–4.06 (m, 28H, 4 × CH and 12 × CH₂, H-5, H-26, H-35, H-74), 3.90 (br s, 18H, 4 × CH₂ and 10 × CH, H-14, H-73), 3.80 (br s, 9H, 4 × CH₂, and CH-a, H-9, H-38a), 3.70–3.67 (m, 6H, CH and CH-b and 4 × CH-a, H-46, H-38b, H-7a), 3.54 (br s, 12H, 4 × CH₂ and 4 × CH-b, H-8, H-7b), 3.31 (br s, 8H, 4 × CH₂, H-53), 3.14–3.08 (m, 10H, 5 × CH₂, H-65), 2.09–2.08 (m, 12H, 4 × CH₃, OCOCH₃), 2.06–2.04 (m, 30H, 10 × CH₃, OCOCH₃), 2.00–1.94 (m, 42H, 14 × CH₃, OCOCH₃), 1.90–1.88 (m, 42H, 14 × CH₃, OCOCH₃), 1.84 (s, 12H, 4 × CH₃, OCOCH₃), 1.82 (s, 6H, 2 × CH₃, OCOCH₃), 1.79 (s, 6H, 2 × CH₃, OCOCH₃), 1.77 (s, 6H, 2 × CH₃, OCOCH₃), 1.53–1.32 (m, 105H, 27 × CH₃ and 12 × CH₂, H-50, H-51, H-52, H-49, H-49'), 1.03 (d, *J* = 6.3 Hz, 12H, 4 × CH₃, H-6), 0.91–0.78 (m, 2H, CH₂-axle), 0.52 (br s, 2H, CH₂-axle), 0.44 (br s, 2H, CH₂-axle), 0.34 (br s, 2H, CH₂-axle), 0.19 (br s, 2H, CH₂-axle), –0.24 (br s, 2H, CH₂-axle), –0.36 (br s, 1H, CH₂-axle), –0.46 (br s, 1H, CH₂-axle), –0.56 (br s, 1H, CH₂-axle), –0.75 (br s, 1H, CH₂-axle). ¹³C NMR (126 MHz, CDCl₃-d₁): δ_C = 173.7, 172.7, 172.3, 172.2 (4 × Cq, C-39, C-41, C-43, C-45), 171.0 (Cq, C-19), 170.5, 170.3, 170.28, 170.2, 170.0, 169.9, 169.4 (52 × Cq, C=O_{acetyl}), 163.5, 163.44, 163.40, 163.36 (4 × Cq, C-54), 157.2 (Cq, C-47), 156.13, 156.1, 156.0, 155.9 (4 × Cq, C-56), 153.2 (4 × Cq, C-55), 149.3, 149.2 (10 × Cq_{Ar}, C-57, C-60), 145.8 (2 × Cq_{triazole}, C-24, C-37), 144.2, 144.1 (10 × Cq, C-67), 144.0, 143.9 (4 × Cq, C-12), 142.9 (Cq_{triazole}, C-17), 142.2 (Cq_{triazole}, C-17'), 135.2 (Cq_{Ar}, C-23), 132.5 (Cq_{Ar}, C-20), 128.9, 128.0 (10 × Cq_{Ar} and 2 × CH_{Ar}, C-59, C-62, C-21), 125.3 (2 × CH_{Ar}, C-22), 123.9 (5 × CH, C-11, C-16), 123.8 (CH, C-16'), 123.4, 123.3, 123.1 (10 × CH, C-66), 122.1 (CH, C-36), 120.2 (CH, C-25), 115.7, 115.5 (10 × CH_{Ar}, C-58, C-61), 100.2, 100.1 (10 × CH, H-69), 96.2 (4 × CH, C-1), 83.1, 83.0, 82.97 (4 × Cq, C-48'), 81.5, 80.2 (CH, C-48), 79.3, 79.2, 79.16, 76.13, 76.10 (4 × Cq, C-48''), 71.0 (4 × Cq, C-4), 70.7 (10 × CH, C-73), 70.6 (10 × CH, C-71), 70.1 (4 × CH₂, C-8), 69.4 (4 × CH₂, C-9), 68.8 (4 × CH₂, C-14), 68.6 (10 × CH, C-70), 68.1 (4 × CH, C-2), 67.8 (4 × CH, C-3), 67.3 (10 × CH₂, C-63, C-63'), 67.2 (4 × CH₂, C-7), 67.0 (10 × CH, C-72), 64.4 (4 × CH₂, C-13), 64.3 (4 × CH, C-5), 62.6, 62.5 (10 × CH₂, C-68), 60.4 (10 × CH₂, C-74), 60.6 (2 × CH, C-15), 56.8 (CH, C-40), 55.3, 54.9, 54.1 (3 × CH, C-42, C-44, C-46), 51.3, 51.1 (14 × CH₂, C-10, C-64, C-64'), 49.8 (CH₂, C-26), 49.3 (CH₂, C-35), 43.7 (CH₂, C-18), 40.7, 40.6, 40.5, 40.4 (4 × CH₂, C-53), 40.1 (CH₂, C-38), 38.9 (CH₂, C-18'), 30.9 (4 × CH₂, C-50), 30.8 (CH₂-axle), 30.3 (CH₂-axle), 30.1 (CH₂-axle), 29.2 (CH₂-axle), 28.8, 28.74, 28.7 (11 × CH₂, C-52, C-65, CH₂-axle), 28.3, 28.21, 28.2, 28.0 (CH₃, C-49, C-49'), 26.1 (CH₂-axle), 25.7 (CH₂-axle), 24.0, 23.7, 23.2, 23.0 (4 × CH₂, C-51), 20.8, 20.6, 20.58, 20.5 (52 × CH₃, OCOCH₃), 15.8 (4 × CH₃, C-6). HRMS (ESI-TOF) (*m/z*): [M + 6H]⁶⁺ Calcd for C₄₀₈H₅₇₂N₇₂O₁₇₃: 1541.3004, requires 1542.1429.

Deca-Galactosylated Hetero[2]rotaxane 5c. The title compound **5c** was prepared using **5b** (0.0075 mmol, 0.040 g), **18** (0.089 mmol, 0.034 g), CuSO₄·5H₂O (0.0037 mmol, 0.0009 g), and sodium ascorbate (0.011 mmol, 0.0022 g) in CH₂Cl₂/H₂O (0.32:0.17 mL) according to general procedure **G** and isolated as a yellow viscous gel that solidified to pale yellow glassy solid (0.0072 mmol, 0.067 g, 99%). Purity is >95%. *R*_f = 0.14 in CH₂Cl₂/MeOH (95:5). ¹H NMR (400 MHz, CDCl₃-d₁): δ_H = 11.48–14.46 (m, 4H, *NHBoc*), 8.32–8.29 (m, 4H, *NH-C=NBoc*), 8.03 (d, *J* = 6.4 Hz, 2H, 2 × CH_{Ar}, H-22), 7.91–7.87 (m, 4H, 2 × CH and 2 × CH_{Ar}, H-16, H-16', H-21), 7.81–7.72 (m, 14H, 14 × CH, H-66, H-11), 7.60 (br s, 1H, CH, H-36), 7.53–7.51 (m, 1H, CH, H-25), 7.39 (br s, 1H, NH), 7.35 (br s,

1H, NH), 7.10 (br s, 1H, NH), 6.72 (br s, 10H, 10 × CH_{Ar} H-58, H-61), 6.55 (br s, 1H, NH), 5.38–5.37 (m, 10H, 10 × CH, H-72), 5.31 (dd, *J* = 10.2, 2.8 Hz, 4H, 4 × CH, H-3), 5.26 (app d, *J* = 2.5 Hz, 4H, 4 × CH, H-4), 5.20–5.13 (m, 10H, 10 × CH, H-70), 5.10–5.07 (m, 8H, 8 × CH, H-1, H-2), 5.02–4.92 (m, 20H, 5 × CH₂ and 10 × CH, H-68, H-71), 4.88 (br s, 2H, 2 × CH, H-15), 4.80–4.62 (m, 52H, 21 × CH₂ and 10 × CH, H-13, H-18, H-18', H-64, H-68', H-69), 4.53 (br s, 8H, 4 × CH₂, H-10), 4.34–4.23 (m, 23H, 3 × CH and 10 × CH₂, H-40, H-42, H-44, H-63, H-63'), 4.14–4.11 (m, 28H, 4 × CH and 12 × CH₂, H-5, H-26, H-35, H-74), 3.97–3.95 (m, 18H, 4 × CH₂ and 10 × CH, H-14, H-73), 3.87 (br s, 8H, 4 × CH₂, H-9), 3.77–3.74 (m, 5H, CH and 4 × CH_{2a}, H-46, H-7a), 3.63–3.59 (br s, 12H, 4 × CH₂ and 4 × CH_{2b}, H-8, H-7b), 3.38 (br s, 10H, 5 × CH₂, H-53, H-38a, H-38b), 3.20, 3.15 (2 s, 10H, 5 × CH₂, H-65), 2.68 (br s, 2H, CH₂, H-79), 2.15 (br s, 12H, 4 × CH₃, OCOCH₃), 2.13–2.11 (m, 30H, 10 × CH₃, OCOCH₃), 2.03–2.01 (m, 42H, 14 × CH₃, OCOCH₃), 1.97–1.95 (m, 42H, 14 × CH₃, OCOCH₃), 1.91 (s, 12H, 4 × CH₃, OCOCH₃), 1.88 (s, 12H, 4 × CH₃, OCOCH₃), 1.84 (s, 6H, 2 × CH₃, OCOCH₃), 1.72–1.42 (m, 109H, 27 × CH₃ and 14 × CH₂, H-50, H-51, H-52, H-49, H-49', H-77, H-78), 1.10 (d, *J* = 6.4 Hz, 12H, 4 × CH₃, H-6), 0.88–0.82 (m, 6H, 3 × CH₂-axle), 0.53 (br s, 2H, CH₂-axle), 0.39 (br s, 4H, 2 × CH₂-axle), –0.30 (br s, 2H, CH₂-axle), –0.64 (br s, 2H, CH₂-axle). ¹³C NMR (126 MHz, CDCl₃-d₁): δ_C = 173.6, 172.5, 171.8, 171.7 (4 × C_q, C-39, C-41, C-43, C-45), 171.0 (C_q, C-19), 170.5, 170.31, 170.3, 170.2, 170.0, 169.9, 169.4 (52 × C_q, C=O_{acetyl}), 163.5, 163.4 (4 × C_q, C-54), 157.2 (C_q, C-47), 156.2, 156.1, 156.0, 155.9 (4 × C_q, C-56), 153.2 (4 × C_q, C-55), 149.4, 149.3 (10 × C_q, C-57, C-60), 147.7 (C_q, C-24), 145.9 (C_q, C-37), 144.23, 144.2 (10 × C_q, C-67), 144.0, 143.9 (4 × C_q, C-12), 143.0 (C_q, C-17), 142.3 (C_q, C-17'), 135.2 (C_q, C-23), 132.5 (C_q, C-20), 128.9 (10 × C_q, C-59, C-62, C-21), 125.2 (2 × CH_{Ar}, C-22), 123.9 (5 × CH, C-11, C-16), 123.7 (CH, C-16'), 123.3, 123.2, 123.1 (10 × CH, H-66), 122.1 (CH, C-36), 120.2 (CH, C-25), 115.8, 115.6 (10 × CH_{Ar}, C-58, C-61), 100.3, 100.2, 100.1 (10 × CH, H-69), 96.2 (4 × CH, C-1), 83.1, 83.0 (4 × C_q, C-48'), 81.6, 80.2 (C_q, C-48), 79.3, 79.2, 79.1, 76.0 (4 × C_q, C-48''), 71.0 (4 × CH, C-4), 70.7 (10 × CH, C-73), 70.6 (10 × CH, C-71), 70.1 (4 × CH₂, C-8), 69.4 (4 × CH₂, C-9), 68.8 (4 × CH₂, C-14), 68.6 (10 × CH, C-70), 68.1 (4 × CH, C-2), 67.8 (4 × CH, C-3), 67.3 (10 × CH₂, C-63, C-63'), 67.2 (4 × CH₂, C-7), 67.0 (10 × CH, C-72), 64.4 (4 × CH₂, C-13), 64.3 (4 × CH, C-5), 62.6, 62.5 (10 × CH₂, C-68), 61.1 (10 × CH₂, C-74), 60.4 (2 × CH, C-15), 56.9 (CH, C-40), 55.4, 54.8, 53.9 (3 × CH, C-42, C-44, C-46), 50.2 (14 × CH₂, C-10, C-64, C-64'), 49.6 (CH₂, C-26), 49.4 (CH₂, C-35), 43.7 (CH₂, C-18), 40.8, 40.6, 40.4, 40.1 (4 × CH₂, C-53), 39.1 (CH₂, C-18'), 39.0 (CH₂, C-38), 30.9 (4 × CH₂, C-50), 30.1 (CH₂-axle), 30.0 (CH₂-axle), 29.3 (2 × CH₂, C-79, CH₂-axle), 29.1 (CH₂-axle), 28.8, 28.74, 28.7 (11 × CH₂, C-52, C-65, C-77, CH₂-axle), 28.3, 28.23, 28.2, 28.0 (CH₃, C-49, C-49'), 26.6 (CH₂-axle), 26.1 (CH₂-axle), 25.9 (CH₂-axle), 25.2 (5 × CH₂, C-52, C-78), 24.1, 23.8, 23.2, 23.0 (4 × CH₂, C-51), 20.8, 20.63, 20.6, 20.5 (52 × CH₃, OCOCH₃), 15.8 (4 × CH₃, C-6). HRMS (ESI-TOF) (*m/z*): [M + 6H]⁶⁺ Calcd for C₄₁₁H₅₇₈N₇₂O₁₇₃: 1547.3004, requires 1546.1505.

Deca-Galactosylated Hetero[2]rotaxane 6c. The title compound **6c** was prepared using **6b** (0.0065 mmol, 0.035 g), **18** (0.078 mmol, 0.030 g), CuSO₄·5H₂O (0.0033 mmol, 0.0008 g), and sodium ascorbate (0.001 mmol, 0.0019 g) in CH₂Cl₂/H₂O (0.29:0.15 mL) according to general procedure **G** and isolated as a yellow viscous gel that solidified to pale yellow glassy solid (0.0065 mmol, 0.060 g, 99%). Purity is >95%. *R*_f = 0.27 in EtOAc/CH₂Cl₂/MeOH (80:10:10). ¹H NMR (500 MHz, CDCl₃-d₁): δ_H = 11.46 (br s, 4H, NHBoc), 8.38 (br s, 4H, NH-C=Nboc), 8.06–8.02 (m, 2H, 2 × CH_{Ar}, H-22), 7.91–7.81 (m, 4H, 2 × CH and 2 × CH_{Ar}, H-16, H-16', H-21), 7.827.73 (m, 14H, 14 × CH, H-66, H-11), 7.54–7.52 (m, 1H, CH, H-36), 7.44 (br s, 1H, CH, H-25), 7.35 (br s, 1H, NH), 7.29 (br s, 1H, NH), 7.17–7.11 (m, 1H, NH), 6.88(d, *J* = 7.6 Hz, 1H, NH), 6.78–6.74 (m, 10H, 10 × CH_{Ar}, H-58, H-61), 5.38 (br s, 10H, 10 × CH, H-72), 5.31 (app d, *J* = 9.8 Hz, 4H, 4 × CH, H-3), 5.26 (br s, 4H, 4 × CH, H-4), 5.19–5.14 (m, 10H, 10 × CH, H-70), 5.10–5.08 (m, 8H, 8 × CH, H-1, H-2), 5.02–5.00 (m, 10H, 10 × CH, H-71),

4.97–4.88 (m, 12H, 2 × CH and 5 × CH₂, H-15, H-68), 4.80–4.72 (m, 30H, 15 × CH₂, H-64, H-68'), 4.69–4.65 (m, 10H, 10 × CH, H-69), 4.62 (br s, 12H, 6 × CH₂, H-13, H-18, H-18'), 4.52 (br s, 8H, 4 × CH₂, H-10), 4.38–4.19 (m, 21H, CH and 10 × CH₂, H-40, H-63, H-63'), 4.13 (br s, 30H, 6 × CH and 12 × CH₂, H-5, H-26, H-35, H-42, H-44, H-74), 3.96 (br s, 18H, 4 × CH₂ and 10 × CH, H-14, H-73), 3.87 (br s, 9H, 4 × CH₂ and CH-a, H-9, H-38a), 3.76–3.73 (m, 6H, CH and CH-b and 4 × CH-a, H-46, H-38b, H-7a), 3.67–3.60 (br s, 12H, 4 × CH₂ and 4 × CH-b, H-8, H-7b), 3.39 (br s, 8H, 4 × CH₂, H-53), 3.19–3.13 (m, 10H, 5 × CH₂, H-65), 2.17 (br s, 6H, 2 × CH₃, OCOCH₃), 2.16 (br s, 12H, 4 × CH₃, OCOCH₃), 2.13–2.12 (m, 30H, 10 × CH₃, OCOCH₃), 2.03–2.01 (m, 36H, 12 × CH₃, OCOCH₃), 1.98–1.86 (m, 42H, 14 × CH₃, OCOCH₃), 1.91 (s, 12H, 4 × CH₃, OCOCH₃), 1.89 (s, 6H, 2 × CH₃, OCOCH₃), 1.87 (s, 6H, 2 × CH₃, OCOCH₃), 1.85 (s, 6H, 2 × CH₃, OCOCH₃), 1.61–1.40 (m, 105H, 27 × CH₃ and 12 × CH₂, H-50, H-51, H-52, H-49, H-49'), 1.11 (d, *J* = 6.4 Hz, 12H, 4 × CH₃, H-6), 0.84–0.80 (m, 6H, 3 × CH₂-axle), 0.63 (br s, 4H, 2 × CH₂-axle), –0.14 (br s, 4H, 2 × CH₂-axle), –0.52 (br s, 2H, CH₂-axle), –0.50 (br s, 2H, CH₂-axle), –0.72 (br s, 2H, CH₂-axle). ¹³C NMR (126 MHz, CDCl₃-d₁): δ_C = 173.6, 172.6, 172.1 (4 × C_q, C-39, C-41, C-43, C-45), 171.0 (C_q, C-19), 170.5, 170.2, 170.1, 170.0, 169.9, 169.4 (52 × C_q, C=O_{acetyl}), 163.3 (4 × C_q, C-54), 157.1 (C_q, C-47), 156.0, 155.9 (4 × C_q, C-56), 153.1 (4 × C_q, C-55), 149.2 (10 × C_q, C-57, C-60), 145.6 (2 × C_q, C-24), 142.9 (C_q, C-37), 144.1 (10 × C_q, C-67), 143.9 (4 × C_q, C-12), 142.9 (C_q, C-17), 142.3 (C_q, C-17'), 135.2 (C_q, C-23), 132.5 (C_q, C-20), 128.8 (10 × C_q, C-59, C-62), 128.5 (2 × CH_{Ar}, C-21), 125.2 (2 × CH_{Ar}, C-22), 123.8 (5 × CH, C-11, C-16), 123.3, 123.2, 123.1 (11 × CH, H-16', H-66), 121.8 (CH, C-36), 119.9 (CH, C-25), 115.7, 115.6 (10 × CH_{Ar}, C-58, C-61), 100.1 (10 × CH, H-69), 96.1 (4 × CH, C-1), 83.0, 82.9 (4 × C_q, C-48'), 81.4 (C_q, C-48), 79.1 (4 × C_q, C-48''), 70.9 (4 × CH, C-4), 70.7 (10 × CH, C-73), 70.6 (10 × CH, C-71), 70.0 (4 × CH₂, C-8), 69.3 (4 × CH₂, C-9), 68.7 (4 × CH₂, C-14), 68.6 (10 × CH, C-70), 68.0 (4 × CH, C-2), 67.8 (4 × CH, C-3), 67.2 (10 × CH₂, C-63, C-63'), 67.1 (4 × CH₂, C-7), 66.9 (10 × CH, C-72), 64.3 (4 × CH₂, C-13), 64.2 (4 × CH, C-5), 62.4, 62.4 (10 × CH₂, C-68), 61.0 (10 × CH₂, C-74), 60.4 (2 × CH, C-15), 56.7 (CH, C-40), 55.2, 54.8, 54.0 (3 × CH, C-42, C-44, C-46), 50.1 (14 × CH₂, C-10, C-64, C-64'), 49.7 (CH₂, C-26), 49.2 (CH₂, C-35), 43.7 (CH₂, C-18), 40.7, 40.5, 40.3 (4 × CH₂, C-53), 40.1 (CH₂, C-38), 39.0 (CH₂, C-18'), 30.8, 30.7 (4 × CH₂, C-50), 30.5 (CH₂-axle), 30.3 (CH₂-axle), 30.0 (CH₂-axle), 29.8 (CH₂-axle), 29.2 (CH₂-axle), 28.6 (10 × CH₂, C-52, C-65, CH₂-axle), 28.5 (CH₂-axle), 28.2, 27.9 (CH₃, C-49, C-49'), 26.5 (CH₂-axle), 25.9 (CH₂-axle), 25.8 (CH₂-axle), 23.9, 23.6, 23.1, 22.9 (4 × CH₂, C-51), 20.7, 20.6, 20.5, 20.4 (52 × CH₃, OCOCH₃), 15.7 (4 × CH₃, C-6). HRMS (ESI-TOF) (*m/z*): [M + 6H]⁶⁺ Calcd for C₄₁₀H₅₇₆N₇₂O₁₇₃: 1545.9722, requires 1546.8131.

General Procedure for the Synthesis of 4–6. To a solution of **4d–6d** (1.0 equiv) in dry CH₂Cl₂ (0.038 M) was added TFA (ratio of CH₂Cl₂/TFA is 1:1). The reaction mixture was stirred at room temperature for 4 h before being concentrated by rotary evaporation under vacuum. The obtained slurry (brown gel) was triturated with Et₂O (3 × 1.5 mL) until a precipitate started to form. Decantation of ether followed by filtration provided an off-white solid, which was dissolved in water and lyophilized overnight to yield the desired rotaxanes **4–6**.

Rotaxane 4. The title compound **4** was prepared using **4d** (0.0057 mmol, 0.040 g) in CH₂Cl₂/MeOH (1:1, 0.30 mL) according to general procedure **I** and isolated as a glassy pale yellow solid (0.0056 mmol, 0.038 g, 99%). Purity is >95%. ¹H NMR (500 MHz, CD₃OD-*d*₄): δ_H = 8.55–7.42 (m, 2H, 2 × CH_{Ar}, H-22), 8.26–8.14 (m, 10H, 10 × CH, H-66), 8.00 (br s, 6H, 6 × CH, H-11, H-16, H-16'), 7.76–7.60 (m, 4H, 2 × CH_{Ar} and 2 × CH, H-21, H-25, H-36), 6.55, 6.40 (2 s, 10H, 10 × CH_{Ar}, H-58, H-61), 5.09 (br s, 20 H, 10 × CH₂, H-68), 4.86 (br s, OH), 4.86–4.74 (m, 56H, 20 × CH₂ and 16 × CH, H-1, H-10, H-13, H-15, H-18, H-18', H-64, H-69), 4.67–3.44 (m, 20H, 5 × CH₂ and 10 × CH, H-70, H-63), 4.59–4.09 (m, 21H, 7 × CH₂ and 7 × CH, H-5, H-26, H-35, H-40, H-42, H-44, H-63'), 3.93–3.46 (m, 69H, 23 × CH₂ and 23 × CH, H-2, H-3, H-4, H-7a, H-7b, H-9, H-14,

H-38a, H-38b, H-46, H-73, H-74), 3.34–3.21 (br s, 36H, 20 × CH and 8 × CH₂, H-8, H-53, H-71, H-72), 3.04 (br s, 10H, H-65), 1.84–1.03 (m, 36H, 4 × CH₃ and 12 × CH₂, H-6, H-50, H-51, H-52), 0.14 (br s, 10H, 5 × CH₂-axle), −0.42 (br s, 4H, 2 × CH₂-axle), −0.78 (br s, 2H, CH₂-axle). ¹³C NMR (126 MHz, CD₃OD-*d*₄): δ_C = 174.0, 171.0, 170.2 (4 × C_q, C-39, C-41, C-43, C-45), 167.9 (C_q, C-19), 165.2–164.6 (m, C_q, C-76), 157.4 (4 × C_q, C-54), 150.4 (10 × C_q_{Ar}, C-57, C-60), 146.5 (2 × C_q_{triazole}, C-24, C-37), 144.8 (16 × C_q, C-12, C-67, C-17, C-17'), 131.4 (2 × C_q_{Ar}, C-20, C-23), 130.1, 129.7 (10 × C_q_{Ar}, C-59, C-62), 128.5 (2 × CH_{Ar}, C-21), 126.6, 126.3 (15 × CH and 2 × CH_{Ar}, C-11, C-16, C-22, C-66), 124.5 (2 × CH, C-25, C-36), 124.0 (CH, C-16'), 119.1 (q, *J* = 306 Hz, C_q, C-75), 116.7 (10 × CH_{Ar}, C-58, C-61), 102.2 (10 × CH, H-69), 99.5 (4 × CH, C-1), 76.0 (10 × CH, C-73), 73.6 (10 × CH, C-71), 72.6 (4 × CH, C-4), 71.5 (10 × CH, C-70), 70.5 (4 × CH₂, C-8), 70.4 (14 × CH, C-2, C-72), 69.4 (4 × CH₂, C-9), 68.9 (4 × CH, C-3), 68.3 (10 × CH₂, C-63, C-63'), 67.6 (8 × CH₂, C-7, C-14), 67.2 (4 × CH, C-5), 64.2 (4 × CH₂, C-13), 62.1 (10 × CH₂, C-68), 61.8 (10 × CH₂, C-74), 60.9 (2 × CH, C-15), 55.0, 54.5, 54.1 (4 × CH, C-40, C-42, C-44, C-46), 51.2 (10 × CH₂, C-64, C-64'), 51.0 (4 × CH₂, C-10), 50.6 (2 × CH₂, C-26, C-35), 41.7, 41.5 (7 × CH₂, C-18, C-18', C-38, C-53), 31.5, 31.4 (4 × CH₂, C-50), 30.8, 30.5 (2 × CH₂-axle), 29.0 (2 × CH₂-axle), 28.3 (11 × CH₂, C-52, C-65, CH₂-axle), 26.3 (2 × CH₂-axle), 23.1, 22.8 (4 × CH₂, C-51), 16.2 (4 × CH₃, C-6). HRMS (ESI-TOF) (*m/z*): [M + 6H]⁶⁺ Calcd for C₂₅₉H₃₉₆N₇₂O₁₀₃: 1027.1311, requires 1027.6356.

Rotaxane 5. The title compound **5** was prepared using **5d** (0.007 mmol, 0.050 g) in CH₂Cl₂/MeOH (1:1, 0.18 mL) according to general procedure **I** and isolated as a glassy mustard solid (0.0056 mmol, 0.038 g, 99%). Purity is >95%. ¹H NMR (500 MHz, CD₃OD-*d*₄): δ_H = 8.27–8.14 (m, 10H, 10 × CH, H-66), 7.98–7.91 (br s, 10H, 6 × CH and 4 × CH_{Ar}, H-11, H-16, H-16', H-21, H-22), 7.83–7.75 (m, 2H, 2 × CH, H-25, H-36), 6.64, 6.45 (2 s, 10H, 10 × CH_{Ar}, H-58, H-61), 4.96 (br s, 20H, 10 × CH₂, H-68), 4.84 (br s, OH), 4.75 (br s, 4H, 4 × CH, H-1), 4.71–4.46 (m, 32H, 15 × CH₂ and 2 × CH, H-10, H-13, H-18, H-18', H-64), 4.30–4.06 (m, 27H, 7 × CH₂ and 13 × CH, H-64', H-26, H-35, H-40, H-42, H-44, H-69), 3.88–3.78 (m, 28H, 14 × CH₂, H-9, H-14, H-38a, H-38b, H-63), 3.75–3.68 (m, 33H, 5 × CH₂ and 23 × CH, H-2, H-3, H-5, H-46, H-63', H-72), 4.64–4.56 (m, 36H, 14 × CH₂ and 4 × CH and 4 × CH-a, H-4, H-7a, H-8, H-74), 3.50–4.47 (m, 14H, 4 × CH-b and 10 × CH, H-7b, H-70), 3.40–4.33 (m, 20H, 20 × CH, H-71, H-73), 3.05 (br s, 18H, 9 × CH₂, H-65, H-53), 2.73 (br s, 2H, CH₂, H-79), 1.84–1.12 (m, 40H, 4 × CH₃ and 14 × CH₂, H-6, H-50, H-51, H-52, H-77, H-78), 0.32 (br s, 2H, CH₂-axle), 0.27 (br s, 2H, CH₂-axle), −0.44 (br s, 2H, CH₂-axle), −0.54 (br s, 2H, CH₂-axle), 0.77 (br s, 4H, 2 × CH₂-axle), −1.03 (br s, 4H, 2 × CH₂-axle). ¹³C NMR (126 MHz, CD₃OD-*d*₄): δ_C = 174.3, 170.5, 169.9 (4 × C_q, C-39, C-41, C-43, C-45), 166.6 (C_q, C-19), 163.8 (q, *J* = 35.5 Hz, C_q, C-76), 157.6 (4 × C_q, C-54), 150.5, 150.4, 150.3 (10 × C_q_{Ar}, C-57, C-60), 148.0 (C_q_{triazole}, C-37), 146.8 (C_q_{triazole}, C-24), 144.7 (16 × C_q, C-12, C-67, C-17, C-17'), 132.8 (C_q_{Ar}, C-23), 131.1 (C_q_{Ar}, C-20), 130.2, 129.9 (10 × C_q_{Ar}, C-59, C-62), 129.1 (2 × CH_{Ar}, C-21), 126.8, 126.6, 126.4 (18 × CH and 2 × CH_{Ar}, C-11, C-16, C-16', C-22, C-25, C-36, C-66), 117.4 (q, *J* = 292 Hz, C_q, C-75), 116.9, 116.8, 116.6 (10 × CH_{Ar}, C-58, C-61), 102.3 (10 × CH, H-69), 99.5 (4 × CH, C-1), 76.2, 76.1 (10 × CH, C-73), 73.7 (10 × CH, C-71), 72.7 (4 × CH, C-4), 71.6 (10 × CH, C-70), 70.6 (4 × CH₂, C-8), 70.5 (14 × CH, C-2, C-72), 69.5 (4 × CH₂, C-9), 69.0 (4 × CH, C-3), 68.4 (10 × CH₂, C-63, C-63'), 67.7 (8 × CH₂, C-7, C-14), 67.3 (4 × CH, C-5), 64.2 (4 × CH₂, C-13), 62.3, 62.1 (10 × CH₂, C-68), 61.9 (10 × CH₂, C-74), 61.3 (2 × CH, C-15), 54.9 (CH, C-40), 54.6, 53.7, 52.9 (3 × CH, C-42, C-44, C-46), 51.4 (10 × CH₂, C-64, C-64'), 51.2 (4 × CH₂, C-10), 50.6 (2 × CH₂, C-26, C-35), 46.1 (CH₂, C-18), 41.8, 41.6 (4 × CH₂, C-53), 39.8 (2 × CH₂, C-18', C-38), 31.5 (4 × CH₂, C-50), 30.7 (2 × CH₂-axle), 30.0 (2 × CH₂-axle), 29.1 (2 × CH₂-axle), 28.9 (CH₂, C-79), 28.4 (10 × CH₂, C-52, C-65, C-77), 26.7 (2 × CH₂-axle), 26.4 (CH₂, C-78), 24.1, 23.2, 22.2 (4 × CH₂, C-51), 16.3 (4 × CH₃, C-6). HRMS (ESI-TOF) (*m/z*): [M + 6H]⁶⁺ Calcd for C₂₆₂H₄₀₂N₇₂O₁₀₃: 1034.1389, requires 1034.6437.

Rotaxane 6. The title compound **6** was prepared using **6d** (0.0055 mmol, 0.039 g) in CH₂Cl₂/MeOH (1:1, 0.29 mL) according to general procedure **I** and isolated as pale brown glassy solid (0.0055 mmol, 0.037 g, 99%). Purity is >95%. ¹H NMR (500 MHz, CD₃OD-*d*₄): δ_H = 8.30–7.79 (m, 22H, 4 × CH_{Ar}, 18 × CH, H-11, H-16, H-16', H-21, H-22, H-25, H-36, H-66), 6.57–6.46 (m, 10H, 10 × CH_{Ar}, H-58, H-61), 5.71 (br s, 20 H, 10 × CH₂, H-68), 5.07 (br s, OH), 4.74–4.53 (m, 56H, 20 × CH₂ and 16 × CH, H-1, H-10, H-13, H-15, H-18, H-18', H-64, H-69), 4.16 (m, 20H, 5 × CH₂ and 10 × CH, H-70, H-63), 3.83–3.42 (m, 90H, 30 × CH₂ and 30 × CH, H-2, H-3, H-4, H-5, H-7a, H-7b, H-9, H-14, H-26, H-35, H-38a, H-38b, H-40, H-42, H-44, H-46, H-63', H-73, H-74), 3.29 (br s, 36H, 20 × CH and 8 × CH₂, H-8, H-53, H-71, H-72), 2.96 (br s, 10H, H-65), 1.65–0.93 (br s, 36H, 4 × CH₃ and 12 × CH₂, H-6, H-50, H-51, H-52), 0.44 (br s, 6H, 3 × CH₂-axle), 0.16 (br s, 8H, 4 × CH₂-axle), −0.47 (br s, 4H, 2 × CH₂-axle), −0.85 (br s, 2H, CH₂-axle). ¹³C NMR (126 MHz, CD₃OD-*d*₄): δ_C = 174.6, 174.3, 173.9 (4 × C_q, C-39, C-41, C-43, C-45), 170.5 (C_q, C-19), 164.1 (q, *J* = 33.7 Hz, C_q, C-76), 157.5 (4 × C_q, C-54), 150.5, 150.4 (10 × C_q_{Ar}, C-57, C-60), 146.9 (2 × C_q_{triazole}, C-24, C-37), 144.8 (16 × C_q, C-12, C-67, C-17, C-17'), 132.7 (2 × C_q_{Ar}, C-20, C-23), 130.1, 129.8 (10 × C_q_{Ar}, C-59, C-62), 129.1 (2 × CH_{Ar}, C-21), 126.8, 126.3, 125.7 (18 × CH and 2 × CH_{Ar}, C-11, C-16, C-16', C-22, C-66, C-25, C-36), 118.0 (q, *J* = 233 Hz, C_q, C-75), 116.6 (10 × CH_{Ar}, C-58, C-61), 102.3 (10 × CH, H-69), 99.5 (4 × CH, C-1), 76.2 (10 × CH, C-73), 73.7 (10 × CH, C-71), 72.7 (4 × CH, C-4), 71.1 (10 × CH, C-70), 70.6 (4 × CH₂, C-8), 70.5 (14 × CH, C-2, C-72), 69.5 (4 × CH₂, C-9), 69.0 (4 × CH, C-3), 68.3 (10 × CH₂, C-63, C-63'), 67.7 (8 × CH₂, C-7, C-14), 67.3 (4 × CH, C-5), 64.3 (4 × CH₂, C-13), 62.1 (10 × CH₂, C-68), 61.9 (10 × CH₂, C-74), 61.3 (2 × CH, C-15), 54.9, 54.6, 53.7 (4 × CH, C-40, C-42, C-44, C-46), 51.3 (10 × CH₂, C-64, C-64'), 51.0 (4 × CH₂, C-10), 50.0 (2 × CH₂, C-26, C-35), 41.8, 41.6 (7 × CH₂, C-18, C-18', C-38, C-53), 31.5 (4 × CH₂, C-50), 30.6 (2 × CH₂-axle), 29.7 (2 × CH₂-axle), 29.2 (2 × CH₂-axle), 28.4 (11 × CH₂, C-52, C-65, CH₂-axle), 26.6 (2 × CH₂-axle), 23.2, 22.2 (4 × CH₂, C-51), 16.3 (4 × CH₃, C-6). HRMS (ESI-TOF) (*m/z*): [M + 6H]⁶⁺ Calcd for C₂₆₁H₄₀₀N₇₂O₁₀₃: 1031.8029, requires 1032.3078.

Rotaxane 2. The title compound **2** was prepared using **2c** (0.0092 mmol, 0.073 g) and NaOMe (0.138 mmol, 0.0075 g) in CHCl₃/MeOH (0.46:0.70 mL, ratio of 1:0.66) according to general procedure **H** and isolated as a yellow viscous gel that solidified to a fluffy pale orange solid (0.0073 mmol, 0.041 g, 79%). Purity is >95%. ¹H NMR (500 MHz, CD₃OD-*d*₄): δ_H = 8.29 (br s, 5H, 5 × CH, H-66), 8.20 (br s, 5H, 5 × CH, H-66'), 8.05 (d, *J* = 8.0, 2H, 2 × CH_{Ar}, H-22), 8.00 (br s, 6H, 6 × CH, H-11, H-16, H-16'), 7.87 (d, *J* = 8.4, 2H, 2 × CH_{Ar}, H-21), 7.73 (br s, 2H, 2 × CH, H-25, H-36), 6.62, 6.53 (2 s, 10H, 10 × CH_{Ar}, H-58, H-61), 5.01–4.96 (m, 21H, CH and 10 × CH₂, H-39, H-68), 4.89 (br s, OH), 4.77 (br s, 4H, 4 × CH, H-1), 4.62–4.50 (m, 23H, 2 × CH and 10 × CH₂ and CH-a, H-15, H-38a, H-64), 4.30–4.18 (31H, 10 × CH and 10 CH₂ and CH-b, H-10, H-13, H-18, H-18', H-38b, H-69), 3.95–3.86 (m, 15H, 2 × CH₂ and 11 × CH, H-26, H-35, H-43, H-72), 3.78–3.66 (m, 75H, 19 × CH and 28 × CH₂, H-2, H-3, H-4, H-5, H-9, H-14, H-40, H-41, H-42, H-63, H-74), 3.51 (br s, 22H, 10 × CH and 4 × CH₂ and 4 × CH-a, H-7a, H-8, H-70), 3.42–3.35 (m, 20H, 20 × CH, H-71, H-73), 3.31 (br s, 4H, 4 × CH-b, H-7b), 3.02 (br s, 10H, 5 × CH₂, H-65), 1.33–1.23 (m, 3H, CH₃, H-44), 1.27–0.79 (m, 12H, 4 × CH₃, H-6), 0.79 (br s, 6H, 3 × CH₂-axle), 0.30, 0.24 (2 s, 2H, CH₂-axle), 0.08 (br s, 2H, CH₂-axle), −0.14 (br s, 4H, 2 × CH₂-axle), −0.39 (br s, 2H, CH₂-axle). ¹³C NMR (126 MHz, CD₃OD-*d*₄): δ_C = 173.7 (C_q, C-19), 150.6, 150.5 (10 × C_q_{Ar}, C-57, C-60), 147.0 (C_q_{triazole}, C-24), 145.1 (10 × C_q_{triazole}, C-67), 144.7 (7 × C_q_{triazole}, C-12, C-17, C-17', C-37), 138.4 (C_q_{Ar}, C-23), 135.8 (C_q_{Ar}, C-20), 132.9 (2 × CH_{Ar}, C-21), 131.1, 130.2 (10 × C_q_{Ar}, C-59, C-62), 129.1 (CH, C-16), 128.5 (2 × CH_{Ar}, C-22), 126.8 (5 × CH, C-11, C-16'), 126.2 (10 × CH, C-66), 125.1 (2 × CH, C-25, C-36), 117.0, 116.7 (10 × CH_{Ar}, C-58, C-61), 102.7 (10 × CH, C-69), 99.7 (5 × CH, C-1, C-39), 76.3, 76.2 (10 × CH, C-73), 73.9 (10 × CH, C-71), 72.8 (5 × CH, C-4, C-42), 71.8 (10 × CH, C-70), 70.73 (4 × CH₂, C-8), 70.70 (5 × CH, C-2, C-43), 69.7 (10 × CH, C-72), 69.6 (4 × CH₂, C-9), 69.2 (6 × CH,

C-3, C-40, C-41), 68.6, 68.4 (10 × CH₂, C-63, C-63'), 67.7 (8 × CH₂, C-7, C-14), 67.4 (4 × CH, C-5), 64.4 (4 × CH₂, C-13), 62.3 (10 × CH₂, C-68), 62.0 (11 × CH₂, C-38, C-74), 61.5 (2 × CH, C-15), 51.4 (10 × CH₂, C-64, C-64'), 51.1 (6 × CH₂, C-10, C-26, C-35), 45.8 (CH₂, C-18), 41.3 (CH₂, C-18'), 31.0 (CH₂-axle), 30.7 (CH₂-axle), 30.3 (CH₂-axle), 29.6 (CH₂-axle), 29.5, 29.3 (5 × CH₂, C-53, C-53'), 28.3 (CH₂-axle), 26.8 (CH₂-axle), 26.5 (CH₂-axle), 16.4 (5 × CH₃, C-6, C-44). HRMS (ESI-TOF) (*m/z*): [M + 5H]⁵⁺ Calcd for C₂₃₇H₃₄₈N₅₅O₁₀₄: 1125.6721, requires 1126.0755.

Rotaxane 3. The title compound **3** was prepared using **3c** (0.0078 mmol, 0.077 g) and NaOMe (0.117 mmol, 0.0063 g) in CHCl₃/MeOH (0.4:0.59 mL, ratio of 1:1.5) according to general procedure **H** and isolated as a yellow viscous gel that solidified to a fluffy pale orange solid (0.0063 mmol, 0.045 g, 81%). Purity is >95%. ¹H NMR (500 MHz, CD₃OD-*d*₄): δ_H = 8.00 (br s, 12H, 12 × CH, H-11, H-16), 7.82–7.71 (m, 16H, 12 × CH and 4 × CH_{Ar}, H-22, H-25, H-66), 7.55–7.36 (m, 4H, 4 × CH_{Ar}, H-21), 6.38, 6.30 (2 s, 10H, 10 × CH_{Ar}, H-58, H-61), 4.67 (br s, OH), 4.54 (br s, 32H, 12 × CH and 10 × CH₂, H-1, H-15, H-68), 4.38–4.27 (m, 42H, 21 × CH₂, H-13, H-10, H-64), 4.06–3.95 (m, 28H, 10 × CH and 9 × CH₂, H-18, H-18', H-64', H-69), 3.74–3.57 (m, 26H, 26 × CH, H-3, H-5, H-72), 3.52–3.40 (m, 104H, 16 × CH and 44 × CH₂, H-2, H-4, H-8, H-9, H-14, H-63, H-74), 3.29 (br s, 26H, 10 × CH and 8 × CH₂, H-7a, H-7b, H-70), 3.16–3.07 (m, 20H, 20 × CH, H-71, H-73), 2.80 (br s, 14H, 7 × CH₂, H-26, H-35, H-65), 0.85 (br s, 24H, 8 × CH₃, H-6), 0.18 (br s, 4H, 2 × CH_{2axle}), 0.09 (br s, 4H, 2 × CH_{2axle}), –0.17 (br s, 4H, 2 × CH_{2axle}), –0.43 (br s, 4H, 2 × CH_{2axle}). ¹³C NMR (126 MHz, CD₃OD-*d*₄): δ_C = 173.8 (2 × C_q, C-19), 150.5, 150.4 (10 × C_{qAr}, C-57, C-60), 146.9 (2 × C_qtriazole, C-24), 144.5 (10 × C_qtriazole, C-67), 144.2 (10 × C_qtriazole, C-12, C-17), 143.4 (2 × C_qtriazole, C-17'), 135.7 (2 × C_{qAr}, C-23), 132.5 (2 × C_{qAr}, C-20), 131.0 (4 × CH_{Ar}, C-20), 130.1, 129.8 (10 × C_{qAr}, C-59, C-62), 129.1 (2 × CH, C-16), 128.5 (4 × CH_{Ar}, C-22), 126.6, 126.5 (18 × CH, C-11, C-66), 125.2 (2 × CH, C-16'), 122.4 (2 × CH, C-25), 116.9, 116.8 (10 × CH_{Ar}, C-58, C-61), 102.6, 102.5 (10 × CH, C-69, C-69'), 99.6 (8 × CH, C-1), 76.2, 76.1 (10 × CH, C-73, C-73'), 73.7 (10 × CH, C-71), 72.7 (8 × CH, C-4), 71.7 (10 × CH, C-70), 70.7 (8 × CH₂, C-8), 70.6 (8 × CH, C-2), 69.6 (10 × CH, C-72), 69.5 (8 × CH₂, C-9), 69.0 (8 × CH, C-3), 68.5, 68.4 (10 × CH₂, C-63, C-63'), 67.7 (16 × CH₂, C-7, C-14), 67.3 (8 × CH, C-5), 64.1 (8 × CH₂, C-13), 62.2 (10 × CH₂, C-68), 61.9 (10 × CH₂, C-74), 61.4 (4 × CH, C-15), 51.3 (18 × CH₂, C-10, C-64, C-64'), 51.0 (2 × CH₂, C-26, C-35), 46.0 (2 × CH₂, C-18), 41.4 (2 × CH₂, C-18'), 30.8 (2 × CH_{2axle}), 29.6 (2 × CH_{2axle}), 29.4 (2 × CH_{2axle}), 29.3 (5 × CH₂, C-65), 26.7 (2 × CH_{2axle}), 16.4 (8 × CH₃, C-6). HRMS (ESI-TOF) (*m/z*): [M + 6H]⁶⁺ Calcd for C₃₀₁H₄₄₄N₇₄O₁₂₈: 1190.5079, requires 1191.1792.

Isothermal Titration Calorimetry (ITC). Recombinant LecA and LecB were produced in *Escherichia coli*, purified by affinity chromatography, dialyzed, and lyophilized as previously described.²⁹ Protein concentration was assessed using Nanodrop 2000 UV–vis spectrophotometer by measurement of absorbance at 280 nm using a theoretical molarity extinction coefficient of 27 960 and 6990 nM^{−1} cm^{−1} for LecA and LecB, respectively. ITC experiments were performed with a VP-ITC isothermal titration calorimeter (Micro-Cal-Malvern). The experiments were carried out at 25 °C. Lectins and ligands were dissolved in the same buffer composed of 20 mM Tris with 100 mM NaCl and 100 μM CaCl₂ at pH 7.5 (5% DMSO final). The protein concentration in the microcalorimeter cell (1.447 mL) varied from 45.4 to 54.0 μM. A total of 30 injections of 13 μL of sugar solution at concentrations varying from 0.125 to 0.300 mM were added at intervals of 5 min while stirring at 310 rpm. Control experiments performed by injection of buffer into the protein solution yielded insignificant heats of dilution. The experimental data were fitted to a theoretical titration curve using Origin software supplied by MicroCal, with Δ*H* (enthalpy change), *K*_a (association constant), and *n* (number of binding sites per monomer) as adjustable parameters. Dissociation constant (*K*_d), free energy change (Δ*G*), and entropy contributions (TΔ*S*) were derived from the previous parameters.

Bacterial Growth with PAO1. Using OD₆₀₀ (optical density at 600 nm), a culture of *Pseudomonas aeruginosa* (PAO1 strain) was grown from the frozen stock in tryptic soy broth (TSB) culture medium for 24 h (overnight) at 37 °C. This culture of bacterial cells was diluted in TSB to an optical density of 0.2 at 600 nm (OD₆₀₀) which contains ~10⁸ CFU/mL. Next, 50 μL of serial 1:2 dilutions of compounds **1–6** in sterilized Milli-Q water >3% DMSO (150, 75, 37.5, 18.8, 9.4, 4.7, 2.4, and 1.2 μM) were prepared in round-bottom 96-well microplates (Costar, Corning). Control wells with bacteria and no compounds (50 μL of sterilized Milli-Q water >3% DMSO and 50 μL of bacterial culture, positive growth control) and wells without bacteria containing sterilized culture TSB medium (100 μL, negative growth control) were also prepared. An equal volume (50 μL, ~5 × 10⁶ CFU) of bacterial suspensions was added to each well with the exception of negative control wells. The edge wells of the plate were filled with Milli-Q sterilized water (100 μL) to reduce the edge-effect.³⁰ After incubation for 24 h at 37 °C, the bacterial growth was determined by recording the optical density at a wavelength of 600 nm using a Tecan plate reader (SpectraMax iD3_Multimode Microplate Reader). Each concentration of compound was tested in six replicates, and three independent experiments were performed. Using the relative OD₅₉₀ (relative optical density at 590 nm), a culture of *Pseudomonas aeruginosa* (PAO1 strain) was grown from the frozen stock in tryptic soy broth (TSB) culture medium for 24 h (overnight) at 37 °C. Growth in the presence of various concentrations of compounds **4–6** was determined using a modified microdilution assay in round-bottom 96-well microtiter plates (Costar, Corning). The inoculum, prepared from this 24 h culture, contained ~10⁶ CFU/mL. Next, 100 μL of serial 1:2 dilutions of compounds **4–6** in sterilized Milli-Q water >3% DMSO (150, 75, 37.5, 18.8, 9.4, 4.7, 2.4 and 1.2 μM) were prepared so that each well of the microtiter plates contained 100 μL of the inoculum (approx. 10⁵ CFU) and 100 μL of the compound in the appropriate concentration. Control wells with bacteria and no compounds (100 μL of sterilized Milli-Q water >3% DMSO and 100 μL of bacterial culture, positive growth control) and wells without bacteria containing sterilized culture TSB medium (200 μL, negative growth control) were also prepared. The edge wells of the plate were filled with Milli-Q sterilized water (100 μL) to reduce the edge-effect.³⁰ After incubation for 48 h at 37 °C, the bacterial growth was determined by measuring the absorbance at a wavelength of 590 nm using an Envision Xcite multilabel counter (PerkinElmer Life and Analytical Sciences, Boston, MA). Experiments were done in duplicate.

Bacterial Growth Curve Analysis with PAO1. To determine growth curves in the presence of heteroglyco[2]rotaxanes **2** and **6**, *P. aeruginosa* PAO1 was first grown overnight in tryptic soy broth (TSB) at 37 °C, standardized to an OD_{590nm} of 0.2, and subsequently diluted 100-fold. This diluted suspension (25 μL) was then combined with the appropriate amount (150, 75, 37.5, 18.8, 9.4, 4.7, 2.4, and 1.2 μM) of each compound diluted in growth medium (final volume: 100 μL) and dispensed in the well of a round-bottom 96-well microtiter plate. Control wells with no compound and wells without bacteria containing each tested concentration of the compounds (blanks) were also prepared. This plate was subsequently placed in a temperature-controlled microtiter plate reader (Envision Xcite, PerkinElmer) at 37 °C, and the growth kinetics were monitored by measuring the optical density at 590 nm every 30 min for 24 h.

Biofilm Inhibition with PAO1. Antibiofilm properties were determined as previously described with minor modifications, using the crystal violet assay,^{14b,25b,c,31} which allows us to quantify biofilm formation and inhibition through staining of total biofilm biomass with crystal violet. Briefly, a culture of *Pseudomonas aeruginosa* (PAO1 strain) was grown from the frozen stock in Tryptic Soy Broth (TSB) culture medium for 24 h (overnight) at 37 °C. This culture of bacterial cells was diluted in TSB to an optical density of 0.2 at 600 nm (OD₆₀₀) which contains ~10⁸ CFU/mL. Next, 50 μL of serial 1:2 dilutions of compounds **1–6** or of reference compounds (**20**, **12** and **13**) in sterilized Milli-Q water + 3% DMSO (150, 75, 37.5, 18.8, 9.4, 4.7, 2.4 and 1.2 μM) were prepared in round-bottom 96-well microplates (Costar, Corning). Control wells with bacteria and no

compounds (50 μL of sterilized Milli-Q water >3% DMSO and 50 μL of bacterial culture, positive growth control) and wells without bacteria containing sterilized culture TSB medium (100 μL , negative growth control) were also prepared. An equal volume (50 μL , $\sim 5 \times 10^6$ CFU) of bacterial suspensions was added to each well with the exception of negative control wells. The edge wells of the plate were filled with Milli-Q sterilized water (100 μL) to reduce the edge-effect. After incubation for 24 h at 37 $^\circ\text{C}$, spent media and free-floating bacteria were carefully removed by pipetting. The wells were rinsed once with 100 μL of sterilized Physiological Saline (PS, 9 g NaCl/L). Next, the biofilm biomass present in the different wells was fixed using pure methanol (100 μL). After 15 min, methanol was removed by turning over the plates which were further air-dried at 37 $^\circ\text{C}$. Then, 0.1% crystal violet (100 μL) was added to each well at room temperature. After 20 min, wells were rinsed with Milli-Q water to remove unbound dye and the plates were air-dried. The bound crystal violet was dissolved by adding 33% acetic acid (150 μL) to each well and shaking the plate for 20 min in a plate rotator at a speed of 500 rpm. Biofilm formation was quantified by measuring the difference between the absorbance of untreated and treated bacterial samples for each tested concentration of the compounds and the absorbance of appropriate blank well at 595 nm using a Tecan plate reader (SpectraMax iD3_Multimode Microplate Reader). The MBIC₅₀ was defined as the minimal concentration at which at least 50% reduction in biofilm formation was measured compared to untreated wells. Each concentration of compound was tested in six replicates, and three independent experiments were performed.

Biofilm Dispersal with PAO1. The ability of compounds 4–6 to disperse already established biofilms of *P. aeruginosa* (PAO1 strain) was determined in a similar way to the previous inhibition assay, with the difference that compounds were added to microplates containing 24 h mature biofilms. To each well of a round-bottom 96-well microplate (Costar, Corning), 50 μL of sterilized Milli-Q water >3% DMSO was added followed by the addition of 50 μL of an overnight bacterial culture (OD₆₀₀ = 0.2, $\sim 5 \times 10^6$ CFU). Control wells without bacteria containing sterilized culture TSB medium (100 μL , negative growth control) were also prepared. Plates were incubated for 24 h at 37 $^\circ\text{C}$ to allow biofilm formation. After 24 h, the wells were carefully emptied by pipetting to remove planktonic cells, rinsed once with sterile PS (100 μL), and refilled with 50 μL of sterilized Milli-Q water >3% DMSO. A premixed solution of Milli-Q water >3% DMSO and compound was added to each well. In the positive growth control wells, 50 μL of sterilized Milli-Q water was added followed by the addition of 50 μL of fresh culture TSB medium, while in the negative growth control ones was added 100 μL of TSB. Next, the plates were reincubated for 24 h at 37 $^\circ\text{C}$. After preestablished biofilms were treated with compounds 1–6, the medium from each well was removed and biofilms were washed once with 100 μL of PS and then fixed with 100 μL of methanol (15 min). Afterward, staining using 0.1% crystal violet was performed following the same previous procedure used for the inhibition assay and the biofilm biomass was evaluated by measuring the difference between the absorbance of untreated and treated bacterial samples for each tested concentration of the compounds and the absorbance of appropriate blank well at 595 nm using a Tecan plate reader (SpectraMax iD3_Multimode Microplate Reader). Each concentration of compound was tested in two replicates, and two independent experiments were performed.

Biofilm Inhibition with *S. aureus* Mu50, *P. aeruginosa* WT PAO1, and *P. aeruginosa* $\Delta\text{lecA}\Delta\text{lecB}$. Biofilm inhibition of heteroglyco[2] rotaxanes 2 and 6 toward *S. aureus* Mu50, *P. aeruginosa* double mutant $\Delta\text{lecA}\Delta\text{lecB}$, and the corresponding wild-type (WT) PAO1 was determined using crystal violet staining, as described before.^{25a} Briefly, cells were grown overnight in tryptic soy broth (TSB, *S. aureus* Mu50 and *P. aeruginosa* WT) or TSB + 60 $\mu\text{g}/\text{mL}$ gentamicin (*P. aeruginosa* $\Delta\text{lecA}\Delta\text{lecB}$), standardized to an OD_{590nm} of 0.2, and subsequently diluted a 100-fold. This suspension (50 μL) was then combined with the appropriate amount of compounds 2 or 6 (150, 37.5, 18.8, 9.4, 4.7, 2.4, and 1.2 μM), diluted in growth medium (final volume: 100 μL), and dispensed in the well of a round-bottom 96-well microtiter plate (Costar,

Corning), which was subsequently incubated at 37 $^\circ\text{C}$. After 24 h, the supernatants were removed, biofilms were rinsed with 100 μL of 0.9% (w/v) NaCl, fixed with methanol, and stained with crystal violet. Crystal violet was subsequently released with acetic acid, and the optical density was measured at 590 nm using a microtiter plate reader (Envision Xcite, PerkinElmer). Each concentration was tested in triplicate.

Cell Toxicity Assay. A metabolic activity assay was performed to evaluate the toxicity of compounds to human cells in culture. Briefly, Human Caucasian lung carcinoma epithelial cells (A549 cells) were cultured in Dulbecco's modified Eagle's medium (DMEM) Glutamax medium supplemented with 10% fetal bovine serum (FBS). Cells were plated in 24-well format (40 000 cells per well) and were grown for 24 h at 37 $^\circ\text{C}$ in 5% CO₂. Compounds 2–6, 12, 13, and 20 were added at final concentrations of 0, 15.625, 31.25, 62.5, 125.0, and 250 μM (solutions contained 0.005% DMSO in sterilized Milli-Q water) to the appropriate wells (500 $\mu\text{L}/\text{well}$). Wells without compounds where only DMSO (0.005%) was added served as controls. Plates were incubated for 24 h at 37 $^\circ\text{C}$ in an atmosphere containing 5% CO₂ (humid oven). Afterward, MTT (3-[4,5-dimethylthiazoyl-2-yl]-2,5-diphenyl tetrazolium bromide) solution in PBS (2.5 mg of MTT/mL of PBS) was added to the medium as a staining solution (500 $\mu\text{L}/\text{well}$). Cells were incubated for 2 h at 37 $^\circ\text{C}$ in 5% of CO₂. In parallel, a lysis solution was prepared using a mixture of 30% sodium dodecyl sulfate (SDS; diluted in distilled water and heated to 37 $^\circ\text{C}$)/N,N-dimethyl formamide (2:1). The pH of the solution was then adjusted to 4.7 by adding a few drops of an acid solution (80% acetic acid/ 1 M HCl, 9:1). Following incubation, the supernatant solution was removed by decantation and the lysis solution was added (1 mL/well). Plates were reincubated overnight at 37 $^\circ\text{C}$ in 5% CO₂ to make sure that all cells have been lysed and homogenized and purple crystals have dissolved. Next, the absorbance of each plate was read at OD = 570 nm using a plate reader xMark Microplate Absorbance Spectrophotometer (Bio-Rad). The percentage of cell viability was calculated as follows: $(A_{\text{treatment}} - A_{\text{blank}})/(A_{\text{control}} - A_{\text{blank}}) \times 100\%$, where A is the absorbance. Experiments were performed in triplicate, and the results were obtained from two independent experiments.

Human Red Blood Cell Hemolysis Assay. Human red blood cells (hRBC) were obtained by centrifugation of 3.5 mL of whole blood collected in citrate tubes, from healthy donors at 2000g for 10 min at room temperature. Plasma was discarded and the pellet was resuspended in 3.5 mL of PBS at room temperature. The washing was repeated three times, and the remaining pellet was resuspended in 3.5 mL of PBS at a final hRBC concentration of 5%. The hRBC suspensions (95 μL) were then incubated with each of the tested compounds 2–6, 12, 13, and 20 (5 μL , C₀ = 1500 μM) for 1, 3, and 24 h at 37 $^\circ\text{C}$ in 5% CO₂ using the double-dilution method in 96-well round-bottom microplates (Corning-Costar or Nunc, polystyrene, untreated) starting at a concentration of 75 μM . Controls on each plate included a negative blank medium control (CTR–, PBS; 95 μL hRBC + 5 μL PBS) and a positive/hemolytic activity control, which induced 100% hemolysis (10% w/v solution of Triton X-100; 95 μL hRBC + 5 μL Triton). Following centrifugation (2000 rpm, 10 min, room temperature), 20 μL of the supernatant was removed and transferred to a new 96-well round-bottom microplate. Drabkin solution (180 μL) was added and plates were incubated again for 15 min at room temperature. Absorbance at 540 nm was measured using a microplate reader (SpectraMax-M2), and the results are expressed as a percentage of hemoglobin (mg/mL) released relative to the positive control (CTR+, Triton X-100). Experiments were performed in triplicate, and the results are an average of experiments in blood samples taken from at least two different donors. It has to be noted that the absorbance resulting from the presence of compounds 2–6 alone was also measured. PBS (95 μL) was incubated with each of the tested compounds 2–6 (5 μL , C₀ = 750 μM) using the double-dilution method in two 96-well round-bottom microplates (Corning-Costar or Nunc, polystyrene, untreated) starting at a concentration of 37.5 μM . Following centrifugation (2000 rpm, 10 min, room temperature), 20 μL of the supernatant was removed and transferred to a new 96-well round-bottom plate. Drabkin solution (180 μL) was

added, and plates were incubated again for 15 min at room temperature. Absorbance at 540 nm was measured using a microplate reader (SpectraMax-M2), and the results are expressed as a percentage of hemoglobin (mg/mL) released relative to the positive control (Triton X-100).

■ ASSOCIATED CONTENT

SI Supporting Information

The Supporting Information is available free of charge at <https://pubs.acs.org/doi/10.1021/acs.jmedchem.1c01241>.

Complete experimental details, detailed synthetic procedures and characterization data of the different building blocks and scaffolds, ITC protocol, and biochemical/biological methods (PDF)

■ AUTHOR INFORMATION

Corresponding Author

Stéphane P. Vincent – Department of Chemistry, Laboratory of Bio-Organic Chemistry – NAMur Research Institute for Life Sciences (NARILIS), University of Namur (UNamur), 5000 Namur, Belgium; orcid.org/0000-0001-6258-9058; Email: stephane.vincent@unamur.be

Authors

Tharwat Mohy El Dine – Department of Chemistry, Laboratory of Bio-Organic Chemistry – NAMur Research Institute for Life Sciences (NARILIS), University of Namur (UNamur), 5000 Namur, Belgium

Ravikumar Jimmidi – Department of Chemistry, Laboratory of Bio-Organic Chemistry – NAMur Research Institute for Life Sciences (NARILIS), University of Namur (UNamur), 5000 Namur, Belgium

Andrei Diaconu – Department of Chemistry, Laboratory of Bio-Organic Chemistry – NAMur Research Institute for Life Sciences (NARILIS), University of Namur (UNamur), 5000 Namur, Belgium; Center of Advanced Research in Bionanoconjugates and Biopolymers “Petru Poni”, Institute of Macromolecular Chemistry of Romanian Academy, 700487 Iasi, Romania

Maude Fransolet – Department of Chemistry, Laboratory of Bio-Organic Chemistry – NAMur Research Institute for Life Sciences (NARILIS), University of Namur (UNamur), 5000 Namur, Belgium

Carine Michiels – Department of Chemistry, Laboratory of Bio-Organic Chemistry – NAMur Research Institute for Life Sciences (NARILIS), University of Namur (UNamur), 5000 Namur, Belgium; orcid.org/0000-0002-9169-1294

Julien De Winter – Department of Chemistry, Laboratory of Organic Synthesis and Mass Spectrometry, University of Mons (Umons), 7000 Mons, Belgium; orcid.org/0000-0003-3429-5911

Emilie Gillon – Centre de recherches sur les macromolécules végétales (CERMAV), University of Grenoble Alpes, CNRS, 38000 Grenoble, France

Anne Imberty – Centre de recherches sur les macromolécules végétales (CERMAV), University of Grenoble Alpes, CNRS, 38000 Grenoble, France

Tom Coenye – Laboratory of Pharmaceutical Microbiology, University of Ghent (UGent), 9000 Ghent, Belgium; orcid.org/0000-0002-6407-0601

Complete contact information is available at: <https://pubs.acs.org/doi/10.1021/acs.jmedchem.1c01241>

Notes

The authors declare no competing financial interest.

■ ACKNOWLEDGMENTS

The authors are grateful to UNamur (Move-In-Louvain grant TMED and FSR grant to AD) and FSR-FNRS (Chargé de Recherche mandate to RJ). A.I. and E.G. thank Labex Arcane/CBH-EUR-GS (ANR-17-EURE-0003) and Glyco@Alps (ANR-15-IDEX02) for support. The UMONS MS laboratory acknowledges the Fonds National de la Recherche Scientifique (F.R.S.-F.N.R.S.) for its contribution to the acquisition of the Waters Synapt G2-Si mass spectrometer and for continuing support. The authors thank Prof. Römer (Freiburg University) for providing the double mutant PAO1 strain.

■ REFERENCES

- (1) Otto, M. Staphylococcus epidermidis—the ‘accidental’ pathogen. *Nat. Rev. Microbiol.* **2009**, *7*, 555–567.
- (2) (a) Beloin, C.; Renard, S.; Ghigo, J. M.; Lebeaux, D. Novel approaches to combat bacterial biofilms. *Curr. Opin. Pharmacol.* **2014**, *18*, 61–68. (b) Abedon, S. T. Ecology of anti-biofilm agents I: antibiotics versus bacteriophages. *Pharmaceuticals* **2015**, *8*, 525–558.
- (3) Mah, T.-F.; Pitts, B.; Pellock, B.; Walker, G. C.; Stewart, P. S.; O’Toole, G. A. A genetic basis for *Pseudomonas aeruginosa* biofilm antibiotic resistance. *Nature* **2003**, *426*, 306–310.
- (4) Francolini, I.; Donelli, G. Prevention and control of biofilm-based medical-device-related infections. *FEMS Immunol. Med. Microbiol.* **2010**, *59*, 227–238.
- (5) Gellatly, S. L.; Hancock, R. E. W. *Pseudomonas aeruginosa*: new insights into pathogenesis and host defenses. *Pathog. Dis.* **2013**, *67*, 159–173.
- (6) (a) Wagner, V. E.; Iglewski, B. H. *P. aeruginosa* biofilms in CF infection. *Clin. Rev. Allergy Immunol.* **2008**, *35*, 124–134. (b) Valentini, M.; Gonzalez, D.; Mavridou, D. A. I.; Filloux, A. Lifestyle transitions and adaptive pathogenesis of *Pseudomonas aeruginosa*. *Curr. Opin. Microbiol.* **2018**, *41*, 15–20.
- (7) (a) Johansson, E. M.; Crusz, S. A.; Kolomiets, E.; Buts, L.; Kadam, R. U.; Cacciarini, M.; Bartels, K. M.; Diggle, S. P.; Camara, M.; Williams, P.; Loris, R.; Nativi, C.; Rosenau, F.; Jaeger, K. E.; Darbre, T.; Reymond, J. L. Inhibition and dispersion of *Pseudomonas aeruginosa* biofilms by glycopeptide dendrimers targeting the fucose-specific lectin LecB. *Chem. Biol.* **2008**, *15*, 1249–1257. (b) Wei, Q.; Ma, L. Biofilm matrix and its regulation in *Pseudomonas aeruginosa*. *Int. J. Mol. Sci.* **2013**, *14*, 20983–21005. (c) Rybtke, M.; Hultqvist, L. D.; Givskov, M.; Tolker-Nielsen, T. *Pseudomonas aeruginosa* biofilm infections: community structure, antimicrobial tolerance and immune response. *J. Mol. Biol.* **2015**, *427*, 3628–3645.
- (8) (a) Kolomiets, E.; Swiderska, M. A.; Kadam, R. U.; Johansson, E. M.; Jaeger, K. E.; Darbre, T.; Reymond, J. L. Glycopeptide dendrimers with high affinity for the fucose-binding lectin LecB from *Pseudomonas aeruginosa*. *ChemMedChem* **2009**, *4*, 562–569. (b) Johansson, E. M. V.; Kadam, R. U.; Rispoli, G.; Crusz, S. A.; Bartels, K.-M.; Diggle, S. P.; Camara, M.; Williams, P.; Jaeger, K.-E.; Darbre, T.; Reymond, J.-L. Inhibition of *Pseudomonas aeruginosa* biofilms with a glycopeptide dendrimer containing D-amino acids. *MedChemComm* **2011**, *2*, 418–420. (c) Michaud, G.; Visini, R.; Bergmann, M.; Salerno, G.; Bosco, R.; Gillon, E.; Richichi, B.; Nativi, C.; Imberty, A.; Stocker, A.; Darbre, T.; Reymond, J.-L. Overcoming antibiotic resistance in *Pseudomonas aeruginosa* biofilms using glycopeptide dendrimers. *Chem. Sci.* **2016**, *7*, 166–182. (d) Kadam, R. U.; Bergmann, M.; Hurley, M.; Garg, D.; Cacciarini, M.; Swiderska, M. A.; Nativi, C.; Sattler, M.; Smyth, A. R.; Williams, P.; Camara, M.; Stocker, A.; Darbre, T.; Reymond, J.-L. A glycopeptide dendrimer inhibitor of the galactose-specific lectin LecA and of *Pseudomonas aeruginosa* biofilms. *Angew. Chem., Int. Ed.* **2011**, *50*, 10631–10635.
- (9) (a) Mitchell, E. P.; Houles, C.; Sudakevitz, D.; Wimmerova, M.; Gautier, C.; Pérez, S.; Wu, A. M.; Gilboa-Garber, N.; Imberty, A.

- Structural basis for oligosaccharide-mediated adhesion of *Pseudomonas aeruginosa* in the lungs of cystic fibrosis patients. *Nat. Struct. Biol.* **2002**, *9*, 918–921. (b) Imberty, A.; Wimmerova, M.; Mitchell, E. P.; Gilboa-Garber, N. Structures of the lectins from *Pseudomonas aeruginosa*: insight into the molecular basis for host glycan recognition. *Microbes Infect.* **2004**, *6*, 221–228.
- (10) Wu, L.; Estrada, O. Z. O.; Bains, M.; Shen, L.; Kohler, J. E.; Patel, N.; Musch, E. B. C. M. W.; Fu, Y.-X.; Jacobs, M. A.; Nishimura, M. I.; Hancock, J. R. T. Recognition of host immune activation by *Pseudomonas aeruginosa*. *Science* **2005**, *774*–777.
- (11) (a) Diggle, S. P.; Stacey, R. E.; Dodd, C.; Camara, P. W. M.; Winzer, K.; et al. The galactophilic lectin, LecA, contributes to biofilm development in *Pseudomonas aeruginosa*. *Environ. Microbiol.* **2006**, *8*, 1095–1104. (b) Chemani, C.; Imberty, A.; de Bentzmann, S.; Pierre, M.; Wimmerová, M.; Guery, B. P.; Faure, K. Role of LecA and LecB lectins in *Pseudomonas aeruginosa*-induced lung injury and effect of carbohydrate ligands. *Infect. Immun.* **2009**, *77*, 2065–2075.
- (12) Fong, J. N. C.; Yildiz, F. H. Biofilm matrix proteins. *Microbiol. Spectrum* **2015**, *3*, 201.
- (13) (a) Sommer, R.; Rox, K.; Wagner, S.; Hauck, D.; Henrikus, S. S.; Newsad, S.; Arnold, T.; Ryckmans, T.; Brönstrup, M.; Imberty, A.; Varrot, A.; Hartmann, R. W.; Titz, A. Anti-biofilm agents against *Pseudomonas aeruginosa*: a structure-activity relationship study of C-glycosidic LecB inhibitors. *J. Med. Chem.* **2019**, *62*, 9201–9216. (b) Meiers, J.; Zahorska, E.; Röhrig, T.; Hauck, D.; Wagner, S.; Titz, A. Directing drugs to bugs: antibiotic-carbohydrate conjugates targeting biofilm-associated lectins of *Pseudomonas aeruginosa*. *J. Med. Chem.* **2020**, *63*, 11707–11724.
- (14) (a) Joseph, R.; Kaizerman, D.; Herzog, I. M.; Hadar, M.; Feldman, M.; Fridman, M.; Cohen, Y. Phosphonium pillar[5]arenes as a new class of efficient biofilm inhibitors: importance of charge cooperativity; the pillar platform. *Chem. Commun.* **2016**, *52*, 10656–10659. (b) Joseph, R.; Naugolny, A.; Feldman, M.; Herzog, I. M.; Fridman, M.; Cohen, Y. Cationic pillararenes potently inhibit biofilm formation without affecting bacterial growth and viability. *J. Am. Chem. Soc.* **2016**, *138*, 754–757.
- (15) Gao, L.; Li, M.; Ehrmann, S.; Tu, Z.; Haag, R. Positively charged nanoaggregates based on zwitterionic pillar[5]arene that combat planktonic bacteria and disrupt biofilms. *Angew. Chem., Int. Ed.* **2019**, *58*, 3645–3649.
- (16) Vincent, S. P.; Buffet, K.; Nierengarten, I.; Imberty, A.; Nierengarten, J.-F. Biologically active heteroglycoclusters constructed on a pillar[5]arene-containing [2]rotaxane scaffold. *Chem. – Eur. J.* **2016**, *22*, 88–92.
- (17) (a) Bernardi, A.; Jiménez-Barbero, J.; Casnati, A.; De Castro, C.; Darbre, T.; Fieschi, F.; Finne, J.; Funken, H.; Jaeger, K.-E.; Lahmann, M.; Lindhorst, T. K.; Marradi, M.; Messner, P.; Molinaro, A.; Murphy, P.; Nativi, C.; Oscarson, S.; Penadés, S.; Peri, F.; Pieters, R. J.; Renaudet, O.; Reymond, J.-L.; Richichi, B.; Rojo, J.; Sansone, F.; Schäffer, C.; Turnbull, W. B.; Velasco-Torrijos, T.; Vidal, S.; Vincent, S.; Wennekes, T.; Zuillhof, H.; Imberty, A. Multivalent glycoconjugates as anti-pathogenic agents. *Chem. Soc. Rev.* **2013**, *42*, 4709–4727. (b) Cecioni, S.; Imberty, A.; Vidal, S. Glycomimetics versus multivalent glycoconjugates for the design of high affinity lectin ligands. *Chem. Rev.* **2015**, *115*, 525–561. (c) Imberty, A.; Chabre, Y. M.; Roy, R. Glycomimetics and glycodendrimers as high affinity microbial anti-adhesins. *Chem.–Eur. J.* **2008**, *14*, 7490–7499. (d) Blanco, J. L. J.; Ortiz Mellet, C.; Garcia Fernandez, J. M. Multivalency in heterogeneous glycoenvironments: hetero-glycoclusters, -glycopolymers and -glycoassemblies. *Chem. Soc. Rev.* **2013**, *42*, 4518–4531.
- (18) (a) Palmioli, A.; Spenrandeo, P.; Polissi, A.; Airoldi, C. Targeting bacterial biofilm: a new LecA multivalent ligand with inhibitory activity. *ChemBioChem.* **2019**, *20*, 2911–2915. (b) Consoli, G. M. L.; Granata, G.; Cafiso, V.; Stefani, S.; Geraci, C. Multivalent calixarene-based fucosyl derivative: a new *Pseudomonas aeruginosa* biofilm inhibitor. *Tetrahedron Lett.* **2011**, *52*, 5831–5834. (c) Smadhi, M.; de Bentzmann, S.; Imberty, A.; Gingras, M.; Abderrahim, R.; Goeckjan, P. G. Expeditive synthesis of trithiotriazine-cored glycoclusters and inhibition of *Pseudomonas aeruginosa* biofilm formation. *Beilstein J. Org. Chem.* **2014**, *10*, 1981–1990. (d) Visini, R.; Jin, X.; Bergmann, M.; Michaud, G.; Pertici, F.; Fu, O.; Pukin, A.; Branson, T. R.; Thies-Weesie, D. M. E.; Kemmink, J.; Gillon, E.; Imberty, A.; Stocker, A.; Darbre, T.; Pieters, R. J.; Reymond, J.-L. Structural insight into multivalent galactoside binding to *Pseudomonas aeruginosa* lectin LecA. *ACS Chem. Biol.* **2015**, *10*, 2455–2462. (e) Ligeour, C.; Vidal, O.; Dupin, L.; Casoni, F.; Gillon, E.; Meyer, A.; Vidal, S.; Vergoten, G.; Lacroix, J.-M.; Souteyrand, E.; Imberty, A.; Vasseur, J.-J.; Chevolut, Y.; Morvan, F. Mannose-centered aromatic galactocusters inhibit the biofilm formation of *Pseudomonas aeruginosa*. *Org. Biomol. Chem.* **2015**, *13*, 8433–8444. (f) Yu, G.; Thies-Weesie, D. M. E.; Pieters, R. J. Tetravalent *Pseudomonas aeruginosa* adhesion lectin LecA inhibitor for enhanced biofilm inhibition. *Helv. Chim. Acta* **2019**, *102*, No. e1900014. (g) Boukerb, A. M.; Rousset, A.; Galanos, N.; Méar, J.-B.; Thépaut, M.; Grandjean, T.; Gillon, E.; Cecioni, S.; Abderrahmen, C.; Faure, K.; Redelberger, D.; Kipnis, E.; Dessein, R.; Havet, S.; Darblade, B.; Matthews, S. E.; de Bentzmann, S.; Guéry, B.; Cournoyer, B.; Imberty, A.; Vidal, S. Antiadhesive properties of glycoclusters against *Pseudomonas aeruginosa* lung infection. *J. Med. Chem.* **2014**, *57*, 10275–10289. (h) Granata, G.; Stracquadiano, S.; Consoli, G. M. L.; Cafiso, V.; Stefani, S.; Geracia, C. Synthesis of a calix[4]arene derivative exposing multiple units of fucose and preliminary investigation as a potential broad-spectrum antibiofilm agent. *Carbohydr. Res.* **2019**, *476*, 60–64. (i) Bücher, K. S.; Babic, N.; Freichel, T.; Kovacic, F.; Hartmann, L. Monodisperse sequence-controlled α -L-fucosylated glycoligomers and their multivalent inhibitory effects on LecB. *Macromol. Biosci.* **2018**, *18*, No. 1800337. (j) Goyard, D.; Thomas, B.; Gillon, E.; Imberty, A.; Renaudet, O. Heteroglycoclusters with dual nanomolar affinities for the lectins LecA and LecB from *Pseudomonas aeruginosa*. *Front. Chem.* **2019**, *7*, 666. (k) Deguise, I.; Lagnoux, D.; Roy, R. Synthesis of glycodendrimers containing both fucoside and galactoside residues and their binding properties to PA-IL and PA-III lectins from *Pseudomonas aeruginosa*. *New J. Chem.* **2007**, *31*, 1321–1331.
- (19) (a) Badjić, J. D.; Nelson, A.; Cantrill, S. J.; Turnbull, W. B.; Stoddart, J. F. Multivalency and cooperativity in supramolecular chemistry. *Acc. Chem. Res.* **2005**, *38*, 723–732. (b) González-Cuesta, M.; Ortiz Mellet, C.; Garcia Fernandez, J. M. Carbohydrate supramolecular chemistry: beyond the multivalent effect. *Chem. Commun.* **2020**, *56*, 5207–5222.
- (20) Muñoz, A.; Sigwalt, D.; Illescas, B.; Luczkowiak, J.; Rodriguez, L.; Nierengarten, I.; Holler, M.; Remy, J.-S.; Buffet, K.; Vincent, S.; Rojo, F. J.; Delgado, R.; Nierengarten, J.-F.; Martín, N. Synthesis of giant globular multivalent glycofullerenes as potent inhibitors in a model of Ebola virus infection. *Nat. Chem.* **2016**, *8*, 50–57.
- (21) (a) Hurley, M. N.; Camara, M.; Smyth, A. R. Novel approaches to the treatment of *Pseudomonas aeruginosa* infections in cystic fibrosis. *Eur. Respir. J.* **2012**, *40*, 1014–1023. (b) Worthington, R. J.; Richards, J. J.; Melander, C. Small molecule control of bacterial biofilms. *Org. Biomol. Chem.* **2012**, *10*, 7457–7474.
- (22) Buffet, K.; Nierengarten, I.; Galanos, N.; Gillon, E.; Holler, M.; Imberty, A.; Matthews, S. E.; Vidal, S.; Vincent, S. P.; Nierengarten, J.-F. Pillar[5]arene-based glycoclusters: synthesis and multivalent binding to pathogenic bacterial lectins. *Chem.–Eur. J.* **2016**, *22*, 2955–2963.
- (23) Rodrigue, J.; Ganne, G.; Blanchard, B.; Saucier, C.; Giguère, D.; Shiao, T. C.; Varrot, A.; Imberty, A.; Roy, R. Aromatic thioglycoside inhibitors against the virulence factor LecA from *Pseudomonas aeruginosa*. *Org. Biomol. Chem.* **2013**, *11*, 6906–6918.
- (24) Sabin, C.; Mitchell, E. P.; Pokorná, M.; Gautier, M. C.; Utille, J. P.; Wimmerová, M.; Imberty, A. Binding of different monosaccharides by lectin PA-III from *Pseudomonas aeruginosa*: thermodynamics data correlated with X-ray structures. *FEBS Lett.* **2006**, *580*, 982–987.
- (25) (a) Peeters, E.; Nelis, H. J.; Coenye, T. Comparison of multiple methods for quantification of microbial biofilms grown in microtiter plates. *J. Microbiol. Methods* **2008**, *72*, 157–165. (b) Azeredo, J.; Azevedo, N. F.; Briand, R.; Cerca, N.; Coenye, T.; Costa, A. R.;

Desvaux, M.; Di Bonaventura, G.; Hebraud, M.; Jaglic, Z.; Kacaniová, M.; Knochel, S.; Lourenco, A.; Mergulhao, F.; Meyer, R. L.; Nychas, G.; Simoes, M.; Tresse, O.; Sternberg, C. Critical review on biofilm methods. *Crit. Rev. Microbiol.* **2017**, *43*, 313–351. (c) Di Bonaventura, I.; Baeriswyl, S.; Capecchi, A.; Gan, B. H.; Jin, X.; Siriwardena, T. N.; He, R. K.; Pompilio, T. A.; Di Bonaventura, G.; van Delden, C.; Javor, S. An antimicrobial bicyclic peptide from chemical space against multidrug resistant Gram-negative bacteria. *Chem. Commun.* **2018**, *54*, 5130–5133.

(26) Durka, M.; Buffet, K.; Iehl, J.; Holler, M.; Nierengarten, J.-F.; Taganna, J.; Bouckaert, J.; Vincent, S. P. The functional valency of dodecamannosylated fullerenes with *Escherichia coli* FimH: towards novel bacterial antiadhesives. *Chem. Commun.* **2011**, *47*, 1321–1323.

(27) (a) Novoa, A.; Eierhoff, T.; Topin, J.; Varrot, A.; Barluenga, S.; Imberty, A.; Römer, W.; Winssinger, N. A LecA ligand identified from a galactoside-conjugate array inhibits host cell invasion by *Pseudomonas aeruginosa*. *Angew. Chem., Int. Ed.* **2014**, *53*, 8885–8889. (b) Donnier-Maréchal, M.; Galanos, N.; Grandjean, T.; Pascal, Y.; Ji, D.-K.; Dong, L.; Gillon, E.; He, X.-P.; Imberty, A.; Kipnis, E.; Dessein, R.; Vidal, S. Perylenediimide-based glycoclusters as high affinity ligands of bacterial lectins: synthesis, binding studies and anti-adhesive properties. *Org. Biomol. Chem.* **2017**, *15*, 10037–10043.

(28) (a) Zhao, Y.; Yu, C.; Yu, Y.; Wie, X.; Duan, X.; Dai, X.; Zhang, X. Bioinspired heteromultivalent ligand-decorated nanotherapeutic for enhanced photothermal and photodynamic therapy of antibiotic-resistant bacterial pneumonia. *ACS Appl. Mater. Interfaces* **2019**, *11*, 39648–39661. (b) Zhao, Y.; Guo, Q.; Dai, X.; Wei, X.; Yu, Y.; Chen, X.; Li, C.; Cao, Z.; Zhang, X. A biomimetic non-antibiotic approach to eradicate drug-resistant infections. *Adv. Mater.* **2019**, *31*, No. 1806024.

(29) Wankhede, K. S.; Vaidya, V. V.; Sarang, P. S.; Salunkhe, M. M.; Trivedi, G. K. Synthesis of novel isoxazole-linked steroidal glycoconjugates—an application of a novel steroidal nitrile oxide. *Tetrahedron Lett.* **2008**, *49*, 2069–2073.

(30) Lundholt, B. K.; Scudder, K. M.; Pagliaro, L. A simple technique for reducing edge effect in cell-based assays. *J. Biomol. Screen.* **2003**, *8*, 566–570.

(31) Vandecandelaere, I.; Van Acker, H.; Coenye, T. A Microplate-based system as in vitro model of biofilm growth and quantification. *Methods Mol. Biol.* **2016**, *1333*, 53–66.